RESEARCH ARTICLE

Botany
American Journal of

First fossil woods and palm stems from the mid-Paleocene of Myanmar and implications for biogeography and wood anatomy

Nicolas Gentis[1] | Alexis Licht[2] | Dario De Franceschi[1] | Zaw Win[3] | Day Wa Aung[4] | Guillaume Dupont-Nivet[5,6] | Anaïs Boura[1]

[1]CR2P, UMR7207, MNHN, Sorbonne Université, CNRS, 57 rue Cuvier, CP 48, 75005 Paris, France

[2]CEREGE, Aix Marseille Université, CNRS, IRD, INRAE, Collège de France, Europole Méditerranéen de l'Arbois, BP 80, 13545 Aix-en-Provence, France

[3]Geology Department, Shwebo University, Sagaing Region, Myanmar

[4]Geology Department, University of Yangon, Pyay Rd, Yangon, Myanmar

[5]Géosciences Rennes, Université de Rennes 1, 35042 Rennes, France

[6]Helmholtz Centre Potsdam, German Research Centre for Geosciences, 14473 Potsdam, Germany

Correspondence
Nicolas Gentis, CR2P, UMR7207, MNHN, Sorbonne Université, CNRS, 57 rue Cuvier, CP 48, 75005 Paris, France.
Email: nicolas.gentis@edu.mnhn.fr

Abstract

Premise: The rise of angiosperm-dominated tropical rainforests has been proposed to have occurred shortly after the Cretaceous–Paleogene transition. Paleocene fossil wood assemblages are rare yet provide important data for understanding these forests and whether their wood anatomical features can be used to document the changes that occurred during this transition.

Methods: We used standard techniques to section 11 fossil wood specimens of Paleocene-age, described the anatomy using standard terminology, and investigated their affinities to present-day taxa.

Results: We report here the first middle Paleocene fossil wood specimens from Myanmar, which at the time was near the equator and anchored to India. Some fossils share affinities with Arecaceae, Sapindales (Anacardiaceae, Meliaceae) and Moraceae and possibly Fabaceae or Lauraceae. One specimen is described as a new species and genus: *Compitoxylon paleocenicum* gen. et sp. nov.

Conclusions: This assemblage reveals the long-lasting presence of these aforementioned groups in South Asia and suggests the early presence of multiple taxa of Laurasian affinity in Myanmar and India. The wood anatomical features of the dicotyledonous specimens reveal that both "modern" and "primitive" features (in a Baileyan scheme) are present with proportions similar to features in specimens from Paleocene Indian localities. Their anatomical diversity corroborates that tropical flora display "modern" features early in the history of angiosperms and that their high diversity remained steady afterward.

KEYWORDS
Cenozoic, diversification, low latitude, Sapindales, Southeast Asia, tropical

Tropical forests are renowned hotspots of biodiversity and concentrate most of the angiosperm diversity (Gentry, 1992; Morley, 2000; Hill and Hill, 2001). The origin of this high diversity, the mechanisms and early chronology of angiosperm diversification in tropical forests are still poorly understood (Hill and Hill, 2001; Mittelbach et al., 2007; Pennington et al., 2015 and references therein). Climate change and ecological disturbance during the Cretaceous–Paleogene (K–Pg) transition might have played a role in the early diversification of angiosperms in rainforests (Jaramillo et al., 2010; Carvalho et al., 2021). Modern tropical rainforests became established in

the next ca. 6 Myr (Carvalho et al., 2021) with an important turnover in floral assemblages recorded in fossil pollen (Morley, 2000; Carvalho et al., 2021).

Fossil woods might also have recorded this biotic turnover and the differential diversification between high and low latitudes (Wheeler and Baas, 2019). Few localities in the world have yielded Paleocene wood specimens (Poole, 2000), and about 43% of all Paleocene fossil woods in the InsideWood database (InsideWood, 2004 on; Wheeler, 2011) are from India, mainly from the Deccan intertrappean beds. The Deccan fossil wood specimens are

dated to the latest Maastrichtian–earliest Paleocene (67–65 Ma according to recent redating of Deccan basalts; Schoene et al., 2019) and located near the equator at that time. Seemingly, their taxonomic diversity (many Malpighiales, Malvales, and Sapindales) is already quite close to modern or Miocene India (Wheeler et al., 2017). The anatomical features of these wood specimens are also surprisingly "modern" in a Baileyan way (Bailey and Tupper, 1918) compared to other paleotropical fossil woods from the same age around the world (Wheeler et al., 2017). Wheeler et al. (2017) proposed that hot, tropical conditions at low latitudes accelerated adaptive xylem evolution to fit the high demands for hydraulic efficiency typical for the tropical lowlands. These observations support the role of the Indian subcontinent as a cradle for many taxa of angiosperms and a "raft" for biotic dispersal between Africa and Asia, supporting the "out-of-India" biogeographical hypothesis (Prasad et al., 2018; Bansal et al., 2022; Bolotov et al., 2022; Sanil et al., 2022). The lack of other early Paleocene fossil wood assemblages in low-latitude South Asia hamper further testing of this hypothesis and raise questions about the temporal continuity of these early angiosperm-dominated forests.

So far, Myanmar has yielded Miocene wood assemblages (Gottwald, 1994; Gentis et al., 2022), late middle Eocene wood (Privé-Gill et al., 2004; Licht et al., 2014, 2015), and wood and palm stem specimens of poorly constrained age (Sahni, 1964;

Prakash, 1965a–c, 1973; Prakash and Bande, 1980; Du, 1988). Here we document a new fossil site dated to the mid Paleocene of Myanmar (ca. 61 million years ago [Ma]), which was close to the equator and to India at that time. We studied 11 specimens (Appendix 1) and compared their anatomy with modern and fossil taxa to better document low-latitude floras in Asia through wood anatomical features and taxonomic diversity in the light of the most recent hypotheses for wood evolution and biogeography.

GEOLOGICAL CONTEXT

The fossil wood material comes from a volcanic tuff from the Paunggyi Formation, a late Maastrichtian–Paleocene geological unit from the Minbu Basin (Figure 1A, B), part of the Paleogene forearc basin of the Burma Terrane (Bender, 1983; Cai et al., 2019). During the late Maastrichtian–Paleocene, the Burma Terrane was part of an active island arc spread across the Neotethys (the Transtethyan Arc, the wider Kohistan-Ladakh Island Arc) and was located at ca. $10 \pm 5°S$ (Figure 1C; Westerweel et al., 2019; Westerweel, 2020). The Paunggyi Formation consists of continental and shallow marine silici- and volcaniclastic deposits sourced from the nearby Burmese volcanic arc (the Wuntho-Popa Arc). These volcaniclastic deposits crop out in many places of Ngape Township
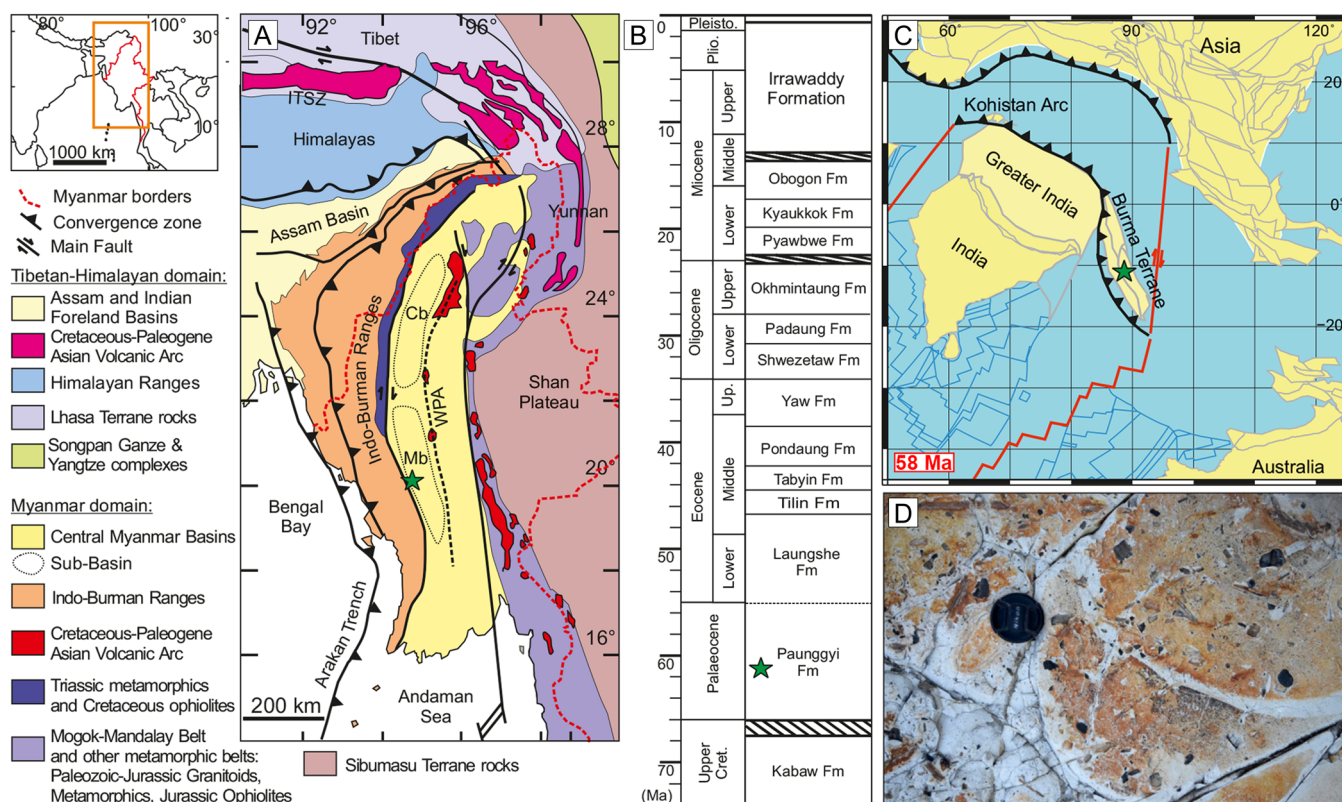
FIGURE 1 (A) Geological map of Myanmar showing the location of the field sites. Green star: location of fossil site. Cb: Chindwin Basin; Mb: Minbu Basin; WPA: Wuntho-Popa Arc (volcanic arc of central Myanmar). (B) Stratigraphy of the Minbu Basin (after Licht et al., 2016). Green star: paleolocation of fossil site. Fm: Formation. (C) Paleogeography of South Asia in the Paleocene, after Westerweel (2020). Green star: fossil site. (D) Tuff layer with isolated pieces of carbonized wood (camera cover diameter: 5 cm).

(Cai et al., 2019). The volcanic tuff yielding fossil woods and palm stems material is north of Ngape along the main road (20°14′25.6″N, 94°20′14.3″E). Fossil material is carbonized and mineralized and found in situ in the tuff layer (Figure 1D) forming a bed of plant debris. The tuff layer was dated by U-Pb zircon geochronology to 61.3 ± 1.6 Ma (early Selandian) at the University of Washington following state-of-the-art extraction and data reduction methods (Appendix S1; methods detailed by Shekut and Licht, 2020). This age directly follows the first pieces of evidence of ophiolite obduction on the Indian passive margin and the accretion of India to the Transtethyan Arc (Ding et al., 2005; Martin et al., 2020). The Paleocene is an epoch characterized by a warm and wet climate with higher average temperatures than today (about 8–10°C warmer) (Zachos et al., 2001, 2008); tropical, subtropical, and paratropical conditions prevailed in addition to temperate, ice-free poles (Akhmetiev, 2007; Williams et al., 2009; Wing et al., 2009). Water availably was regionally variable, and arid or semi-arid zones might have been present with some degree of seasonality (Zachos et al. 2008). In Asia, tropical climate was present near the equator (northern India and South-East Asia) and drier climate in southern India and Central-East China (Quan et al., 2014; Bhatia et al., 2023). Beside the Paleocene–Eocene Thermal Maximum, the Paleocene is also marked by short hyperthermal climatic events characterized by abrupt increases in temperature that could have altered the environmental conditions and changed seasonality and vegetation types in some areas (Speijer, 2003; Bernaola et al., 2008; Hyland et al., 2015; Jehle et al., 2015). The first hyperthermal events, during the Thanetian, postdate the age of the studied fossil bed (Gradstein et al., 2020).

MATERIALS AND METHODS

Eleven specimens of fossil wood from the Paunggyi Formation were collected in 2018 (20°14′25.6″N, 94°20′14.3″E). They are small lignified fragments from 0.9 to 4.6 cm long and were found in situ in the volcanic tuffs. Transverse sections (Ts), tangential longitudinal sections (Tls), and radial longitudinal sections (Rls) of the fossil wood specimens were prepared using standard techniques (Hass and Rowe, 1999) at the Muséum national d'Histoire naturelle (MNHN), Paris, France. Fossils were all embedded and glued with Araldite AY 103 (Huntsman Advanced Materials, Basel, Switzerland) and covered with Araldite 2020 (Huntsman Advanced Materials). Wood anatomy is described following the IAWA lists of microscopic features for hardwood identification (IAWA Committee, 1989) and the list of anatomical features for palm stems from Thomas (2011a) and Thomas and De Franceschi (2013). Pit diameters were measured horizontally. The minimum stem diameter was roughly estimated on the slides using the average geometrical intersection of the rays to locate a virtual center (De Franceschi et al., 2008; Dufraisse et al., 2020) and ranges from 3 to 16.5 cm and is frequently under 10 cm, which means some of the fragments may represent juvenile wood. Botanical affinities were determined

using the InsideWood database (InsideWood, 2004 onward; Wheeler, 2011; Wheeler et al., 2020) and literature on fossil (Gregory et al., 2009) and references therein. For most of the specimens, we first searched the InsideWood database for affinities using a small list of obviously present features. Using an Excel spreadsheet, we then extracted the resulting potential matches and used combinations of features (e.g., scanty OR vasicentric paratracheal parenchyma) to manually filter out any with ambiguous characters. This approach yielded a wider range of potential botanical affinities, that are discussed and compared with the fossils. Additionally, we described each specimen in IAWA Feature codes as is done on InsideWood (the numbers correspond to the IAWA features, with "v" for the variable presence of the feature and "?" for the uncertain presence of the feature). Features that are numbered in the 300's are unique to the fossil wood database. All microscopic slides were deposited in the MNHN (Appendix 1). The remains of the original specimens are to be sent back to the collection of the Department of Geology at the University of Yangon (Myanmar) and are temporarily stored at the MNHN until they can be safely returned to their country of origin. Dicototyledenous specimens are individually described and separated in three groups: (1) multiseriate rays; (2) uni-biseriate rays, (3) scalariform perforations.

RESULTS

The assemblage includes 11 distinct taxa. Two were identified to the family level, five have proposed affinities to the family level, two to the order level, and two are incertae sedis.

Monocotyledons

Order—Arecales Bromhead
    Family—Arecaceae Bercht. & J.Presl
    Subfamily—Arecoideae Burnett or (?) Coryphoideae Burnett
    Genus—*Palmoxylon* Schenk
    Palmoxylon sp.1 (Figure 2)
    Material—Slides MNHN.F.50226.1 to MNHN.F.50226.3 (field number of original specimen: PPP3)
    Repository—Slides: plant fossil collection of the MNHN, Paris. Remains of original specimen: pending restitution to the collection of the Department of Geology at the University of Yangon (Myanmar)
    Locality—Ngape Township, Minbu District, Magway Region, Myanmar
    Age and stratigraphic position—Mid-Paleocene (Danian-Selandian), 61.3 ± 1.6 Ma, Paunggyi Formation
    Description—This specimen is a fragment of stem (3.8 cm long [L] × 1.5 cm wide [l] × 1.0 cm high [H]) lignified and laterally compressed. Likely near the central zone because of the vaguely oriented fibrovascular bundles (fvb) and the markedly spheroid shape of the parenchyma cells. No epidermis nor cortex zone are recognized.

Cocos-Type stem organization: (1) the density of the fibrovascular bundles, d(fvb), is constant throughout the section, d(fvb): 43–57 fvb/cm² (mean 49/cm²); (2) the fibrous vascular surface area ratio, f/v (f = surface area of the fibrous part; v = surface area of the vascular part), is constant throughout the section, f/v: 0.68–2.05 (mean 1.48); (3) the fibrous covering index R (or FCI) (defined as the ratio $R = a/A$ with a = the surface area of the fibrous part of all the fvb in an examined transverse section and A = the whole surface of this area) is almost regular throughout the section, R 0.092–0.133 (mean 0.115). The shape of the fvb is round, and the fibrous dorsal cap appears reniforma (Figure 2A–C). The fvb have the following mean

dimensions: H_{max} = 680 µm, l_{max} = 615 µm, H_{vasc} = 405 µm, l_{vasc} = 410 µm. Fibrous bundles are absent. Auricular sinus absent (or possibly weakly rounded) (Figure 2B, C). No fibrous part adjacent to the xylem is visible (Figure 2B, D, E). Vascular bridges are absent. Vascular zone excluded with mostly 1 vessel element per fvb (sometimes 2) (Figure 2A–C), vessel diameter 170–335 µm (mean 250 µm). Only one phloem strand (Figure 2A–C). Radiating and tabular parenchyma are absent (Figure 2B, C). Phytoliths are globular echinate and abundant throughout the central cylinder (Figure 2F, G), 17–21 µm in diameter (mean 19 µm). The ground parenchyma is spheroid and compact or with small lacunae (Figure 2A–C, G), parenchyma cell diameter of 51–139 µm (mean 88 µm). The

FIGURE 2 *Palmoxylon* sp.1 (Arecaceae). (A–C) MNHN.F.50226.1, transverse sections; (D–G) MNHN.F.50226.3, tangential longitudinal sections. (A) Arrangement of fibrous-vascular bundles (fvb) in a mostly spheroid-compact ground parenchyma with some small lacunae and the beginning of a leaf trace (arrowhead). Boxes outline the area detailed in B and C. (B, C) A fvb with reniforma fibrous dorsal cap. Phloem cells are missing, the perivascular parenchyma is developed. Mostly one vessel element is present in each fvb (arrowheads: bars of scalariform perforations). (D) "Oblique" scalariform perforation with 20 bars on average, surrounded by perivascular parenchyma. (E) Perivascular parenchyma and vessel-parenchyma pits. (F) Globular echinate phytoliths. (G) Globular echinate phytoliths (arrowheads) surrounding the fibers of a fibrous dorsal cap, spheroid (to slightly elongated cells) and compact ground parenchyma on each side. Scale bars: (A) 1 mm; (B–E, G) 200 µm; (F, 25 µm).

scalariform perforations of the end wall of vessels have 20 bars on average, and the slope is "oblique" (end wall length 3 times the end wall width in average) (Figure 2D).

Affinities and remarks

The anatomy of this fossil is characteristic of the Arecaceae, with the presence of the typical fibrovascular bundles (fvb) and phytoliths. Although the arrangement of fvb and ground parenchyma suggests a central zone, it is still uncertain due to the small size of the specimen. As a consequence, some critical features of fossil palms cannot be estimated such as the general stem pattern or the possible secondary growth of some cells. This fossil is described with a Cocos-Type stem organization by default because the size of the specimen limits the possible size variation of the fvb. Some taxa can be dismissed as potential modern analogues using the online identification key Palm-ID (Thomas, 2011b) or comparison with individual features for each subfamily mentioned by Thomas and De Franceschi (2013, table 2: Calamoideae, Nypoideae, Ceroxyloideae, Coryphoideae; Arecoideae are not in the table). The most discriminating feature is the number of wide metaxylem elements per fvb, 1(2) in this fossil (Figure 2A–C). This feature is frequent in the subfamilies Arecoideae and Calamoideae and in some Coryphoideae. Considering the ground parenchyma as spheroid and compact (Figure 2A–C, G) further restricts the results. The closest analogues are found in Arecoideae and Coryphoideae-Borasseae-Lataniinae. The anatomy of the Arecoideae is less extensively studied; because it is the largest subfamily in Arecaceae, the diversity of stem anatomy is also large. Spheroid, compact parenchyma is found in many tribes with Cocosae having in addition one vessel element near the periphery and two vessel elements near the center of the cylinder. Coryphoideae-Borasseae-Lataniinae mostly have a Corypha-Type stem organization, reniforma to lunaria fibrous part; the perivascular parenchyma is well developed as in our fossil (it looks more like parenchyma than fibers as seen in tangential section, Figure 2D, E), phytoliths are abundant but the parenchyma sometimes has slightly elongated cells with small lacunae. We thus suggest a potential affinity with Arecoideae or Coryphoideae-Borasseae.

Few fossil palm stems are known from Myanmar, although palm pollen is commonly found (Huang et al., 2020 for instance). Sahni (1964) described five species from imprecisely described localities and dates (Oligo-Miocene or Mio-Pliocene of the Pegu-Irrawaddy groups), but none are similar to our taxa because the ground parenchyma is never spheroid-compact and radiating, or tabular parenchyma is present. Numerous fossil palm stems have been described from India. More than 82 species are referred as *Palmoxylon* (e.g., Bonde, 2008). Among them, the vast majority are from the Deccan intertraps or dated to the Cretaceous. Few have mostly one vessel element and spheroid-compact to slightly lacunar ground parenchyma. But all these features often vary from the cortex to the central zone. *Palmoxylon sinuosum* Sahni and *P. megalosiphon* Sahni (Sahni, 1964) have fvb similar to the present fossil, but parenchyma cells are less round in *P. sinuosum* and much too lacunar to be

P. megalosiphon. All other *Palmoxylon* from India greatly differ from the present specimen.

Order—Arecales Bromhead
Family—Arecaceae Bercht. & J.Presl
Subfamily—Coryphoideae Burnett or (?) Arecoideae Burnett
Genus—*Palmoxylon* Schenk
Palmoxylon sp.2 (Figure 3)
Material—MNHN.F.50227.1 to MNHN.F.50227.4 (field number of original specimen: PPP4)
Repository—Slides: plant fossil collection of the MNHN, Paris. Remains of original specimen: pending restitution to the collection of the Department of Geology at the University of Yangon (Myanmar)
Locality—Ngape Township, Minbu District, Magway Region, Myanmar
Age and stratigraphic position—Mid-Paleocene (Danian-Selandian), 61.3 ± 1.6 Ma, Paunggyi Formation
Description—This specimen is a fragment of lignified stem (5.2 cm L × 3.6 cm l × 2.5 cm H) and locally compressed. A side difference in the size of the fibrous part between the inner portion and the outer portion (Figure 3A) suggests it is part of the central and transitional zones. No epidermis was recognized. Identified as Corypha-Type stem organization: (1) the density of the fibrovascular bundles, d(fvb), does not significantly vary throughout the section, d(fvb): 95–150 fvb/cm² (mean 124/cm²), $d(fvb)_{out}/d(fvb)_{in}$ = 1,15; (2) the fibrous vascular surface ratio, f/v, is more variable throughout the section, f/v: 0.20–3.68 (8.38) (mean 1.25), $(f/v_{out})/(f/v_{in})$ = 3.74; (3) the fibrous covering index is almost regular throughout the section, R: 0.174–0.195 (mean 0.164), R_{out}/R_{in} = 1.47. The shape of the fvb is generally round, and the fibrous dorsal cap appears reniforma (to complanata?) (Figure 3B, C). The fvb have the following average dimensions: H_{max} = 540 μm, l_{max} = 431 μm, H_{vasc} = 312 μm, l_{vasc} = 345 μm. Possible fibrous part centrifugal differentiation. Fibrous bundles are absent. Raphide sacs present (Figure 3D–F), 14–28 μm in diameter (mean 20 μm), 38–353(860)/cm² (although not all preserved), containing 125–140 needle-shaped crystals. Auricular sinuses are likely absent. No fibrous part is visible adjacent to the xylem. Vascular bridges are absent. Vascular zone excluded, with mostly two vessel elements per fvb (sometimes 3, 4 or more) (Figure 3A–C), vessel diameter 120–334 μm (mean 226 μm). Only one phloem strand. Radiating and tabular parenchyma not visible. Phytoliths are globular echinate and abundant throughout the central cylinder, 14–28 μm of diameter (mean 20 μm) (Figure 3G, H). The ground parenchyma type is likely globular in the inner part or with lacunae and compressed or tangentially elongated cells in the outer part (Figure 3A–D), still with some round lacunae that could be enlarged parenchyma cells that used to contain raphides. The scalariform perforations average 5 cross bars (from 3 to 10), and the slope is "slightly oblique" (end wall length 1–1.3 times the end wall width in average) (Figure 3I).

Affinities and remarks

As for *Palmoxylon* sp.1, the anatomy of this fossil is characteristic of the Arecaceae. However, its preservation state
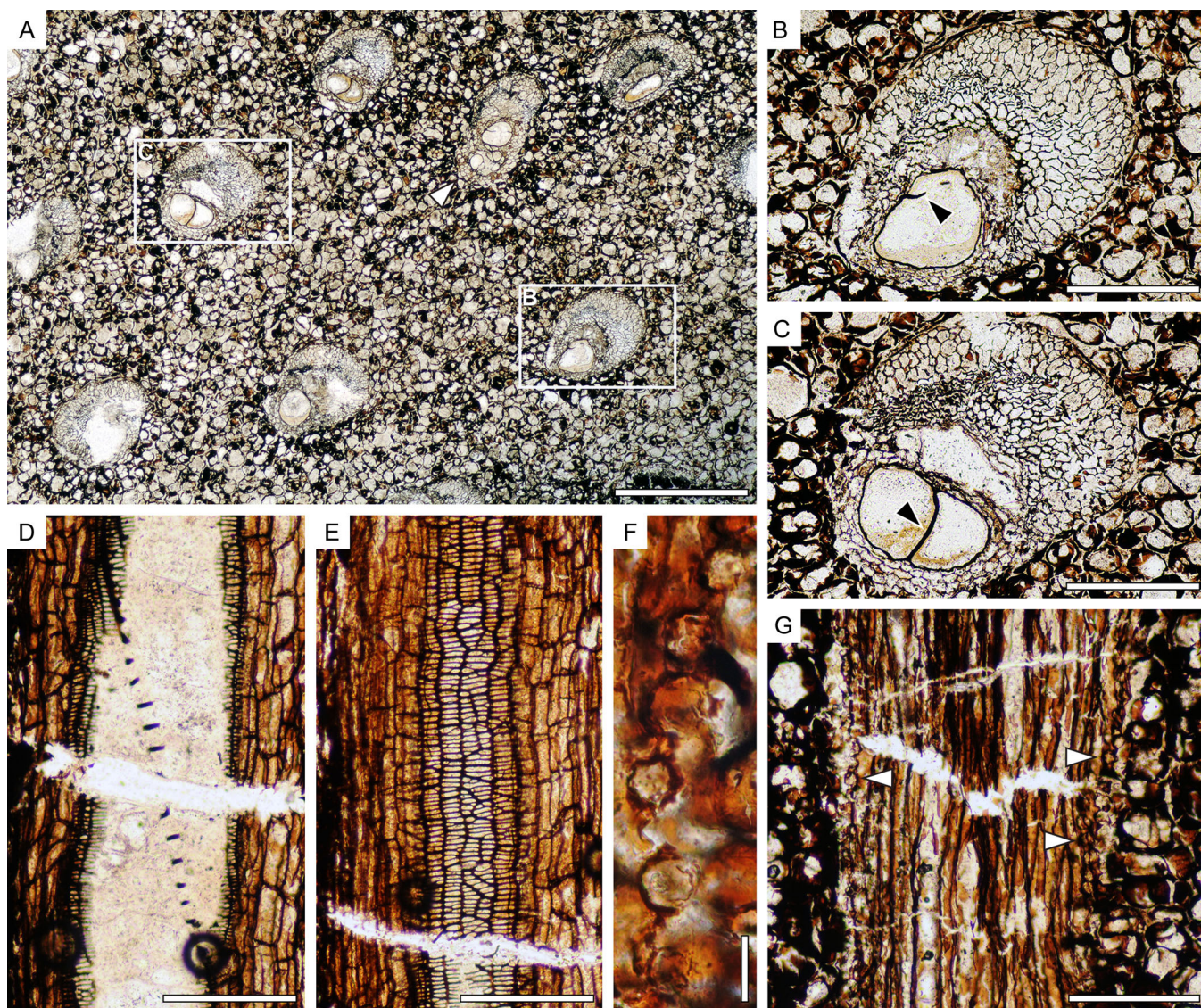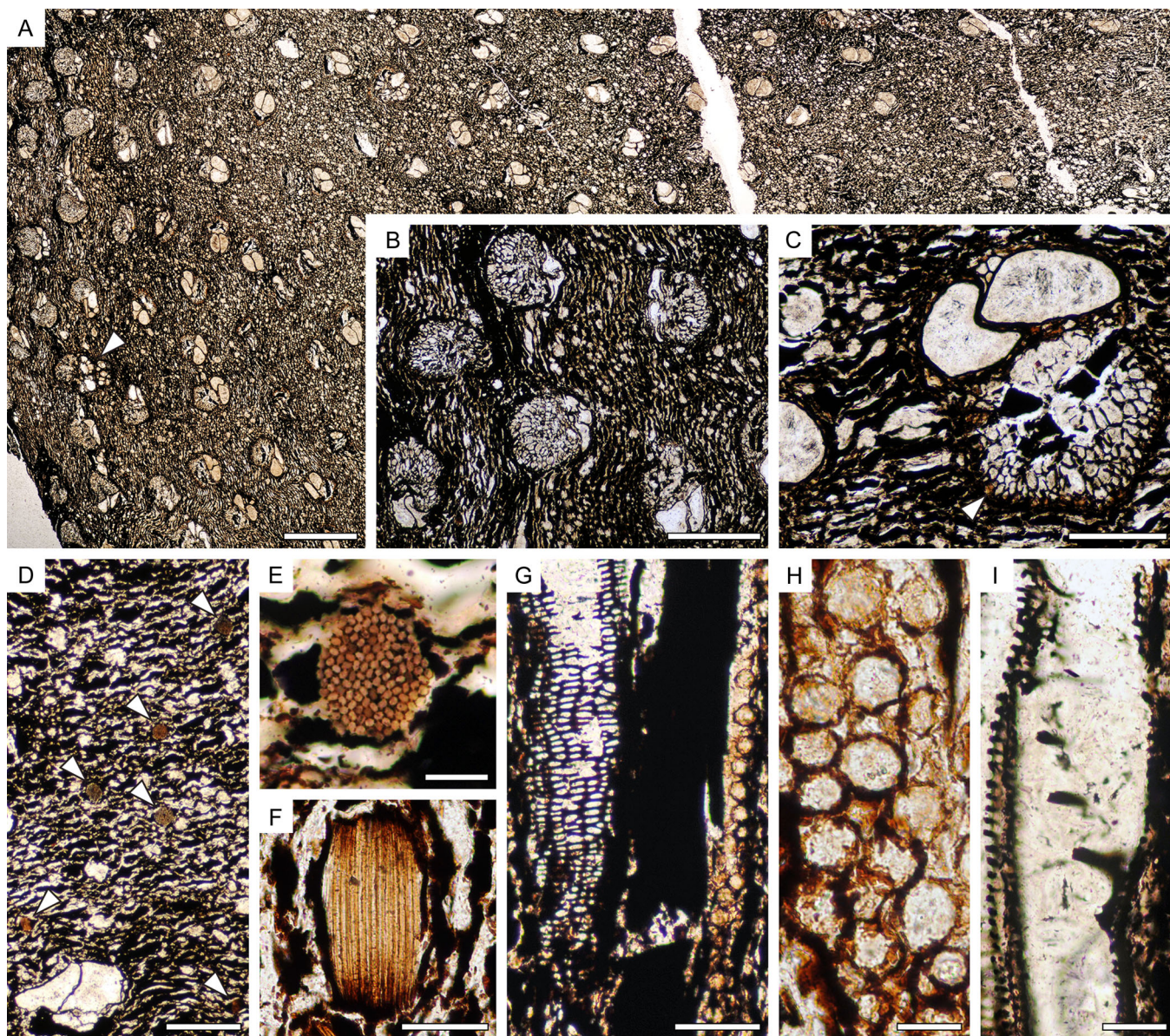
FIGURE 3 *Palmoxylon* sp.2 (Arecaceae). (A–E) MNHN.F.50227.1, transverse sections; (F–I) MNHN.F.50227.4, tangential longitudinal sections. (A) Transitional or subcortical zone with fibrous-vascular bundles (fvb) showing developed dorsal fiber caps (left) and central cylinder with poorly developed dorsal fiber caps (right) and mostly two vessels per fvb; leaf traces regularly visible (arrowhead). (B) Detail of fvb with round dorsal fibrous cap in compressed or tangentially arranged parenchyma. (C) A fvb with two vessel elements, few perivascular parenchyma and stegmata all around the fibrous part containing the phytoliths (arrowhead), compressed or tangentially arranged parenchyma all around. (D) Raphide sacs (arrowheads). (E) Detail of a raphide sac with needle-like crystalline raphides. (F) Longitudinal view of raphides. (G) Vessel-parenchyma pits (left) and globular echinate phytoliths (right). (H) Abundant globular echinate phytoliths. (I) "Slightly oblique" scalariform perforation plates with 5 bars on average. Scale bars: (A) 1 mm; (B) 500 µm; (D) 250 µm; (C) 200 µm; (G) 100 µm; (F, I) 50 µm; (E, H) 25 µm.

does not allow us to precisely assess the nature of the ground parenchyma and all the details of the fibrovascular bundles. It is likely that the area with most-developed fibrous part and relatively frequent leaf traces (Figure 3A) is the "subcortical" or "transition" zone. As for *Palmoxylon* sp. 1, we dismissed some taxa as potential modern analogues using the online identification key Palm-ID (Thomas, 2011b) or by comparisons with each subfamily mentioned by Thomas and De Franceschi (2013). The combined features of our fossil suggest an affinity to the subfamily Coryphoideae, especially with the tribe Borasseae-Hyphaeninae, Sabaleae and Trachycarpeae (especially regarding the type of fibrous part, the nature and arrangement of phytoliths, and the average number of vessel elements). Some tribes of the subfamily Arecoideae have two vessel elements depending on the climate conditions or the position of the fvb in the cylinder. This subfamily is the largest of the Arecaceae, and little information about its stem anatomy is available (see *Palmoxylon* sp.1). Thus, Arecoideae cannot totally be dismissed. One feature is quite remarkable in our specimen: the abundance of raphide sacs (Figure 3D–F).

However, no comprehensive study has yet included raphides in a comparative study of palm stems, so we cannot rely on this trait to help with identification. It is a very variable feature (Tomlinson et al., 2011) found in Coryphoideae, Ceroxyloideae, and Arecoideae (Zona, 2004) or supposedly more common in the stipes of Arecoideae (Cocosae) than Coryphoideae (Thomas, 2011a).

As for *Palmosylon* sp.1, we had difficulty finding a fossil species that matched the features of our specimen. Raphides are never described, although rare idioblasts are mentioned for *P. scottii* Dayal & Menon or *P. pondicherriense* Sahni (Sahni, 1943; Menon, 1964). Although many species have mostly two vessel elements per bundle, only *P. scleroder-mum* has vessels with a relatively larger size compared to the fibrous part, close to each other, separated by one or two rows of parenchyma cells (Sahni, 1943). But it is also described with a Mauritia-Type stem organization, and the paratracheal parenchyma is more developed than in our fossil. Our comparison falls short because the arrangement of the parenchyma in our specimen was difficult to assess.

Dicotyledons

Group 1: Multiseriate rays

Wood-type 1-a (Figure 4)
Affinity—Sapindales (Meliaceae) or Fabales? (Fabaceae?)

Material—MNHN.F.50228.1 to MNHN.F.50228.6 (field number of original specimen: PPP0)

Repository—Slides: plant fossil collection of the MNHN, Paris. Remains of original specimen: pending restitution to the collection of the Department of Geology at the University of Yangon (Myanmar)

Locality—Ngape Township, Minbu District, Magway Region, Myanmar

Age and stratigraphic position—Mid-Paleocene (Danian-Selandian), 61.3 ± 1.6 Ma, Paunggyi Formation

Description—Wood diffuse-porous. Growth ring boundaries faint, marked by marginal parenchyma bands, 3–4 cells wide (Figure 4A), a change of the vessel diameter, change of fiber radial diameter (Figure 4C, J) and less confluent parenchyma close to growth ring boundary. Vessels mostly solitary (70%) or in pairs (30%), rarely in 3's; evenly distributed, oval to round in cross-sectional outline, 1–4/mm² (mean 2/mm²); tangential diameter 75–220 μm (mean 130 μm) (Figure 4B); radial diameter 93–200 μm (mean 144 μm). Tyloses not observed. Vessel element length 188–307 μm (mean 252 μm). Perforation plates simple. Intervessel pits alternate, minute to small, 3–6 μm wide (mean 4 μm) (Figure 4I). Vessel-ray pits similar in size and shape to intervessel pits (Figure 4H). Axial parenchyma predominantly confluent to banded (Figure 4A, B). These bands are paratracheal, wavy, sometimes discontinuous or anastomosed; 1–6 cells wide (mostly 3–4 cells), 2–7 bands/mm (mean 4); otherwise aliform parenchyma with long, thin wings; also in a vasicentric sheath 2–4 cells thick; parenchyma cells 50–127 μm (mean 87 μm) long, 10–40 μm (mean 23 μm) wide; 2–4 cells per parenchyma strand, probably up to 5–6 cells; crystals present in chambered axial parenchyma cells (Figure 4E), up to 10 crystals per strand, 15–45 μm (mean 26 μm) of diameter. Rays fusiform, 1–5-seriate, mostly 3–4-seriate (Figure 4D–E), (1-seriate: 10%, 2-seriate: 23%, 3-seriate: 33%, 4-seriate: 32%, 5-seriate: 3%), 5–8(9) rays/mm (mean 7/mm), 95–580 μm (mean 280 μm) or 4–29 cells (mean 13 cells) high, uniseriate rays about 4–8 cells high; heterocellular to weakly heterocellular with procumbent body cells and mostly 1 marginal row of square (or larger procumbent) cells (Figure 4F). Kribs's ray type heterogeneous IIB (faintly homogeneous I). End-to-end connections rare; square cells might have contained crystals. Fibers non-septate, 9–28 μm in tangential diameter (mean 17 μm) (Figure 4C), walls partially visible in radial section, mostly arranged in radial rows, distinct pits on radial walls 2.5–5.6 μm of diameter (mean 4.2 μm), simple or minutely bordered (Figure 4G).

Estimated minimal diameter—5–6 cm

Description in InsideWood codes (fossil code in parentheses)—2 5 13 22 24 25 30 42 46 52 61? 62? 66 79 80 82 83 85 86 89 92 93v 97v 98 106 115 136 137? 142 168 (301 302 307? 308 313 315)

Affinities and remarks

This specimen is characterized by (1) diffuse-porous wood, (2) confluent to banded axial parenchyma, (3) abundant crystals in chambered parenchyma, (4) heterocellular rays with one row of marginal cells, (5) at least 4 cells per parenchyma strand, (5) 1–5-seriate rays, (6) vessel density less than 5/mm², (7) vessel-ray pits similar to intervessel pits. In addition, the presence of distinctive fiber pits is noteworthy, as are the tendency to ring boundaries marked by changes in vessel diameter, fiber radial diameter, spacing between parenchyma bands and marginal parenchyma (Figure 4A–C, J). Searching InsideWood (2004 onward) with various combinations of the above characters consistently yields family Fabaceae and the order Sapindales. Most species of Fabaceae have vestured pits, which are not seen in this fossil; however, the observation of vestures is uncertain (Wheeler et al., 2020). The few Fabaceae with non-vestured pits, in subfamilies Dialioideae, Duparquetioideae, and Cercidoideae (LPWG, 2017) are not similar to the present fossil (Gasson et al., 2003; Inside-Wood, 2004 onward). Fabaceae with vestured pits, larger than 3-seriate heterocellular rays, more than 2 cells per parenchyma strand, banded parenchyma and non-storied features are mostly found in the Detarioideae subfamily (Gasson et al., 2003; InsideWood, 2004 onward), but they also commonly display secretory canals (*Prioria* Griseb., *Detarium* Juss.) or regular bands (*Cynometra* L.). Considering the anatomical diversity among Fabaceae, this family cannot be totally dismissed.

The Sapindales are well documented, both in phylogeny (APG IV, 2016; Muellner-Riehl et al., 2016) and wood anatomy (e.g., Pace et al., 2022). Kirkiaceae, Burseraceae,
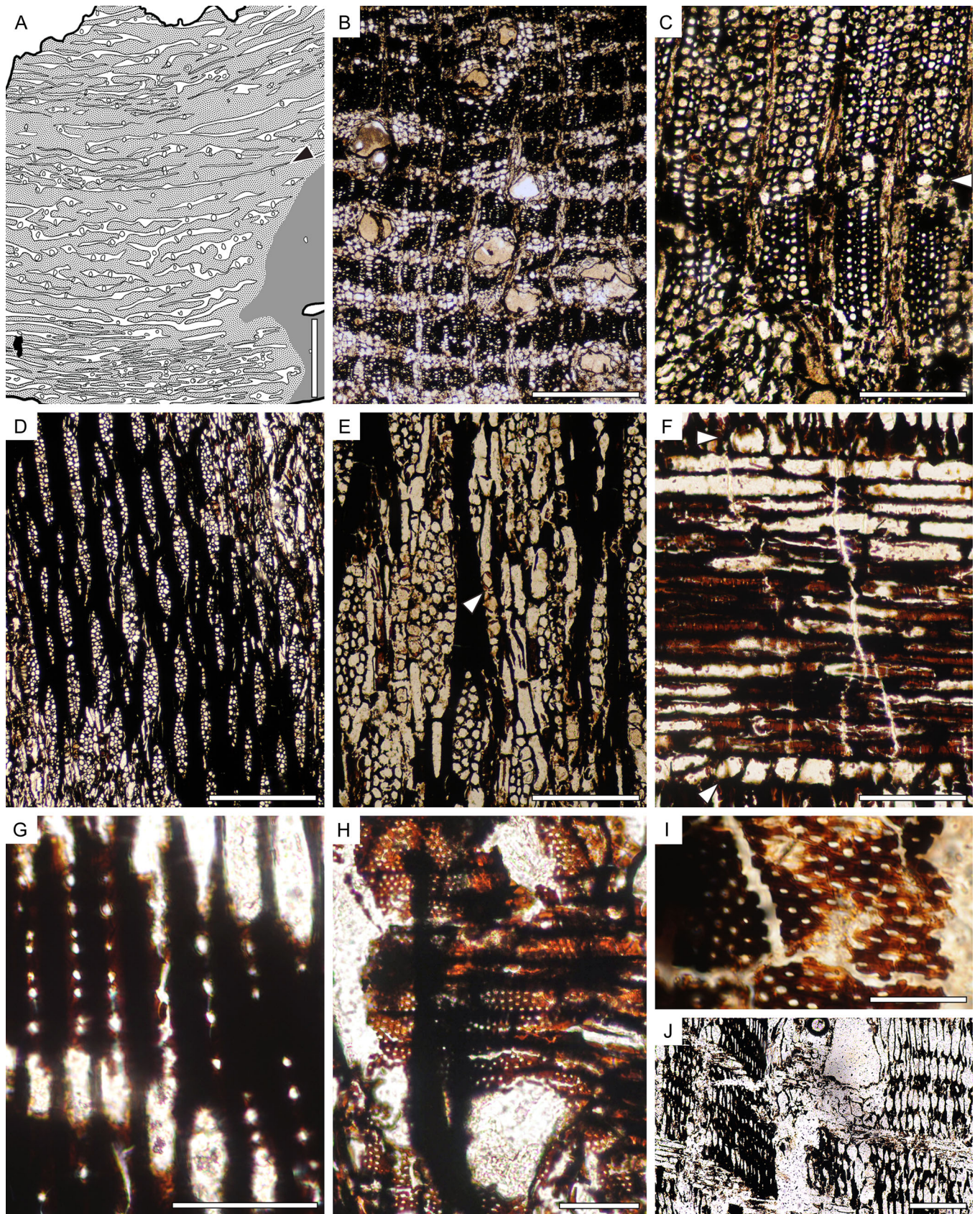
FIGURE 4   (See caption on next page).

and Anacardiaceae differ from our fossil in having large intervessel pits and vessel-ray pits with reduced borders. Among the remaining families, Meliaceae is the most convincing, having small to minute intervessel pits and predominantly paratracheal axial parenchyma, in some genera confluent to banded, axial parenchyma is often crystalliferous (Metcalfe and Chalk, 1950; InsideWood, 2004 onward). Meliaceae include two subfamilies that are distinctive phylogenetically and anatomically (Pennington and Styles, 1975; InsideWood, 2004 onward; Heads, 2019): Some Cedreloideae are similar to this fossil (*Lovoa* Harms, *Neobeguea* J.-F.Leroy, *Entandrophragma* C.DC.) in ray width being mostly more than 3-seriate, but differ in having less paratracheal parenchyma and crystals mainly in ray cells; some Melioideae resemble our fossil (*Guarea* Allemão ex L., *Heynea* Roxb., *Sandoricum* Cav., *Owenia* F.Muell.) because of frequent confluent and crystalliferous parenchyma, but their rays are mainly 1–2-seriate. We thus suggest that this fossil may belong to the Meliaceae and is possibly phylogenetically close to the Melioideae (near the node at the base of Melioideae and Cedreloideae splitting). Alternate affiliations would be close to the Fabaceae.

Among fossils related to Dialioideae and Cercidoideae, the genus *Tzotziloxylon* Pérez-Lara & Estrada-Ruiz (Pérez-Lara et al., 2019) covers fossils sharing features of both subfamilies which include non-vestured intervessel pits, aliform to occasionally confluent axial parenchyma as well as diffuse and sometimes banded up to 3-cells thick, 1–4-seriate rays, crystalliferous axial parenchyma and a non-storied structure. The present fossil has more frequent confluent and banded axial parenchyma that is over 3 cell layers thick and rays larger on average than the two species described in the genus (Pérez-Lara et al., 2019). Other genera such as *Bauhinia* Plum. ex L., *Bauhinium* Trivedi & Panjwani, *Dialioxylon* Lemoigne, Beauchamp & Samuel, *Dialiumoxylon* (Lemoigne & Beauchamp) Lemoigne and *Koompassioxylon* Kramer differ for one or more of these features: storied rays (also parenchyma strands and vessel elements), thinner rays (1–3-seriate), regularly spaced bands of axial parenchyma or wider intervessel pits (6–8 μm) (Ramanujam and Rao, 1966; Kramer, 1974; Lemoigne et al., 1974; Lemoigne, 1978; Guleria, 1984; Trivedi and Panjwani, 1986; Awasthi and Prakash, 1987; Awasthi and Mehrotra, 1990).

Fossils related to Meliaceae are diverse in their anatomy and frequently vary in axial parenchyma abundance and in ray distribution and structure (Appendix S2), but all have paratracheal axial parenchyma, and their intervessel pits are almost always described as minute to small (3–6 μm). Confluent/banded, vasicentric parenchyma and 3(or more)-seriate rays are found in the genera *Carapoxylon* (Mädel) Gottwald with marginal and banded parenchyma and exclusively septate fibers and *Entandrophragminium* Prakash with mostly marginal and vasicentric parenchyma (Prakash, 1976; Gottwald, 1997; Selmeier, 1999). Several species have traumatic canals, unlike this specimen. A review of most species described under these two genera (as well as several other close genera) is provided in the Appendix S2. It reveals a continuum of individual differences unrelated to specific genera that suggest inter- or intraspecific variation rather than intergeneric differences. As mentioned by Pennington and Styles (1975) intrageneric variations are sometimes more striking than intergeneric variations in Meliaceae, especially in the arrangement of axial parenchyma. *Entandrophgrama* is a good example, having parenchyma ranging from scanty paratracheal to almost exclusively banded. Pending a comprehensive review of fossil Meliaceae wood, it seems appropriate to solely consider it as a member of the Sapindales, most likely with the Meliaceae and with some resemblance to *Entandrophragminium* and *Carapoxylon*.

Wood-type 1-b (Figure 5)

Affinity—Rosales (Moraceae) or Sapindales? (Anacardiaceae?, Kirkiaceae?)

Material—MNHN.F.50229.1 to MNHN.F.50229.6 (field number of original specimen: PPP9)

Repository—Slides: plant fossil collection of the MNHN, Paris. Remains of original specimen: pending restitution to the collection of the Department of Geology at the University of Yangon (Myanmar)

Locality—Ngape Township, Minbu District, Magway Region, Myanmar

Age and stratigraphic position—Mid-Paleocene (Danian-Selandian), 61.3 ± 1.6 Ma, Paunggyi Formation

Description—Wood diffuse-porous. Growth-ring boundaries indistinct. Vessels solitary (68%) and in radial multiples of 2–3, occasionally 4–6 (Figure 5A, B), solitary and non-compressed vessels are round to slightly oval in outline (Figure 5C), values for vessel density vary with position in the slide and the state of preservation, 4–23/mm² (mean 12/mm²) (Figure 5A), tangential diameter 44–184 μm (mean 96 μm). Tyloses present in some vessels (Figure 5D). Vessel elements 150–350 μm long (mean 225 μm). Perforations simple (Figure 5K). Intervessel pits

FIGURE 4 Wood-type 1-a (Meliaceae, Fabaceae?). (B, C) MNHN.F.50228.1, transverse sections; (D, E) MNHN.F.50228.3, tangential longitudinal sections; (F–J) MNHN.F.50228.5, radial longitudinal sections. (A) Line drawing of the transverse section highlighting the confluent to banded parenchyma and aliform parenchyma with one band, which might be marginal parenchyma (arrowhead). (B) Detail of the vessels with confluent-banded and aliform parenchyma. (C) Detail of growth-ring boundary with marginal parenchyma (arrowhead) and radially narrowed fibers. (D) Mostly 3–4-seriate fusiform rays. (E) Rays (3–4-seriate) and parenchyma with crystals in chambered cells (arrowhead). (F) Rays with 1 marginal row of square or upright cells (or enlarged procumbent cells) (arrowheads). (G) Simple fiber pits. (H) Vessel-ray pits similar to intervessel pits. (I) Minute to small non-vestured intervessel pits. (J) Growth boundary as in (C) with a difference between fibers with a small radial diameter (left) and larger radial diameter (right). Scale bars: (A) 2.5 mm; (B, D) 500 μm; (C, E) 200 μm; (F, J) 100 μm; (G, H) 50 μm; (I) 20 μm.
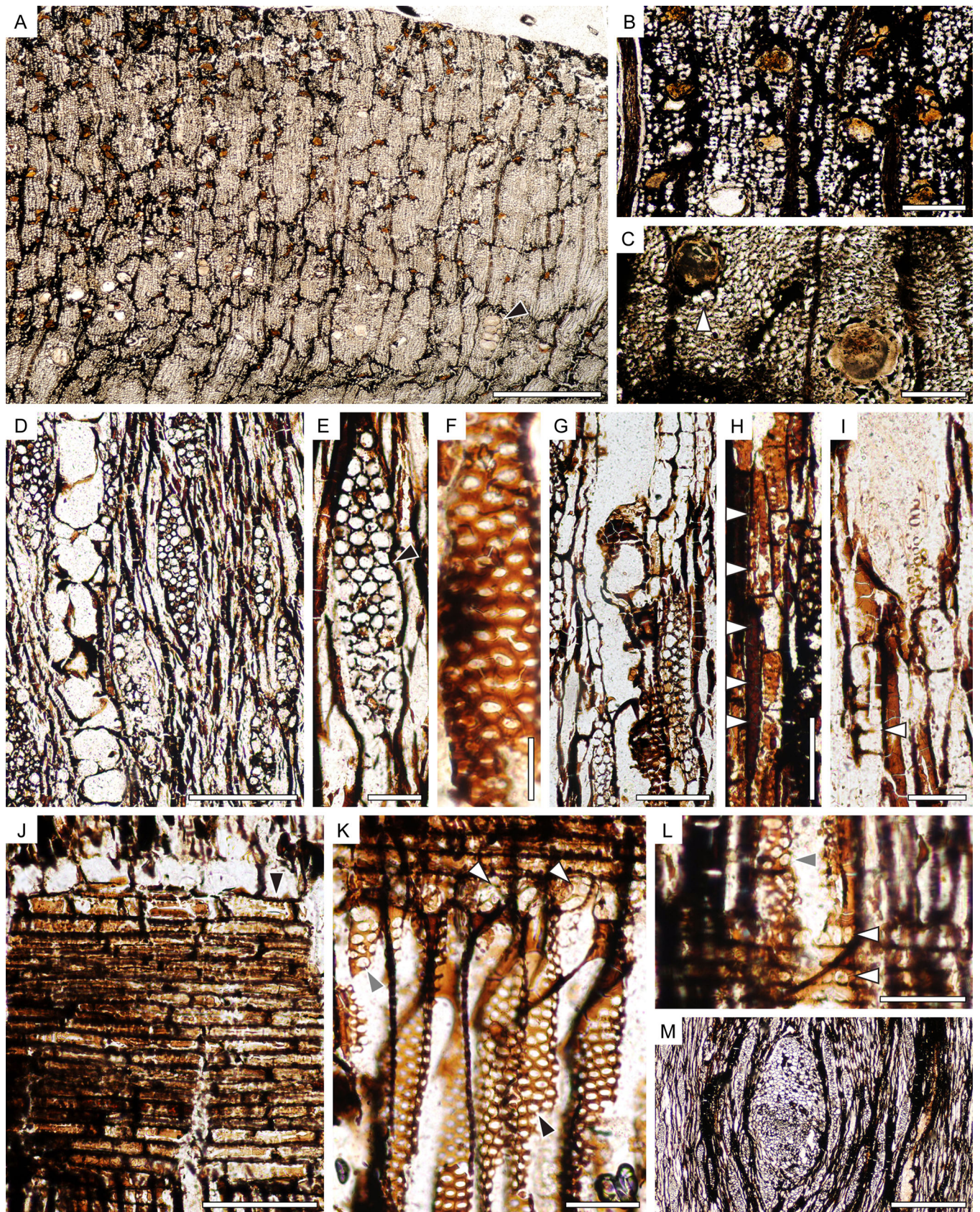
FIGURE 5 (See caption on next page).

alternate, crowded but only slightly polygonal in outline, 5.6–12 μm (mean 8.6 μm) long, non-vestured with large ellipsoidal to lenticular apertures (Figure 5F, K). Vessel-ray parenchyma pits of variable shapes with reduced borders or apparently simple, 5.3–14.5 μm (mean 8.7 μm) large (Figure 5K, L). Vessel-axial parenchyma pits almost of the same size as intervessel pits but with a reduced border, larger lenticular aperture and less crowded (Figure 5K, L). Parenchyma indistinct in transverse section (Figure.5C), visible in longitudinal sections as vasicentric (Figure 5G), perhaps diffuse or aliform as well, up to 5(9) cells per strand (Figure 5H), some cells look subdivided (Figure 5I), but this could also be a form of degradation. Axial parenchyma cells 37–133 μm (mean 70 μm) long and 12–35 μm (mean 22 μm) wide in tangential section (Figure 5H). Rays 1–5(–6-)seriate, mostly 2–4-seriate (1-seriate: 3%, 2-seriate: 22%, 3-seriate: 39%, 4-seriate: 31%, 5-seriate: 5%) (Figure 5D, E), 2–6/mm (mean 4/mm), ray height 82–614 μm (mean 265 μm) or 5-40 cells (mean 17 cells) high; rays heterocellular with procumbent body cells with 1(–2) marginal row(s) of either square/upright or enlarged procumbent cells (Figure 5J). Kribs's ray type heterogeneous IIB to homogeneous I. Intercellular spaces sometimes visible in tangential section between ray cells (Figure 5E). Mean length to height ratio of the procumbent cells of 4.7, with abundant small pits at the edges of the cells (Figure 5J). Fibers seemingly non-septate, arranged in radial rows, 11–29 μm in tangential diameter (mean 20 μm), thin-to-thick walled (lumen about 1 time the double-wall thickness). One small branch trace present in tangential section (Figure 5M).

Estimated minimal diameter—between 7 and 16 cm

Description in InsideWood codes (fossil code in parentheses)—5 13 22 26 27v 31 41 42? 47 52 56v 65? 66 69 76? 79 80? 83? 92 93 97 98 104? 106 114 115 136 142 168 (300 302 308 313 315)

Affinities and remarks

This wood is characterized by (1) simple perforation plates, (2) medium to large, alternate intervessel pits, (3) vessel-ray parenchyma pits with reduced borders or simple, (4) parenchyma mostly paratracheal, (5) rays commonly >3-seriate, (6) rays heterocellular with procumbent body cells and a few marginal rows of square/upright cells, (7) vessel element length short to medium, (8) tyloses present. These features are all present and commonly occur in Moraceae (Metcalfe and Chalk, 1950; Koek-Noonnan et al., 1984a, b; ter Welle et al., 1986a, b; InsideWood, 2004 onward; Ogata et al., 2008), but not found all together in a single genus or

species. A few differences can be pointed out. Vessels with an average diameter <100 μm is not a common character among Moraceae (22%, InsideWood, 2004 onward), nor is vessel density over 20/mm² (about 16%, InsideWood, 2004 onward). Moraceae commonly have an average vessel diameter between 100–200 μm and a vessel density between 5 and 10/mm². The tribe Moreae gather some of the genera that share common features with the present fossil: crystals in chambered axial parenchyma, absence of laticifer (e.g., *Batocarpus* H. Karst., *Prainea* King ex Hook.f., *Trophis* P.Browne, *Streblus* Lour., *Maclura* Nutt.) that is otherwise a common feature of the family. Intercellular space between ray cells (Figure 5E) occur in some Moraceae (*Antiaris* Lesch., *Parartocarpus* Baill.) and in some Malvaceae, Euphorbiaceae, and Fabaceae Ogata et al. (2008). It is also seen in some Combretaceae and Sapotaceae (D. De Franceschi, personal observation). For fossil woods, this feature might not have diagnostic value because it is difficult to determine whether it is a genuine feature of the specimen or a result of taphonomy. Beside Moraceae, some combinations of features present in our fossil are suggestive of other families: Anacardiaceae (thinner rays, uniseriate more common), Kirkiaceae (rare or scanty paratracheal parenchyma), and Cannabaceae, Malvaceae, Lamiaceae, Euphorbiaceae, or even Lauraceae that lack oil cells.

Anacardiaceae and Kirkiaceae are phylogenetically close (Muellner-Riehl et al., 2016), but Kirkiaceae only have rare or scanty paratracheal parenchyma. Several Anacardiaceae have radial canals, and many have common uniseriate rays (InsideWood, 2004 onward). Diffuse-porous wood, rays >3-seriate, and no radial canals (InsideWood, 2004 onward): *Antrocaryon* Pierre, *Buchanania* Spreng., *Dracontomelon* Blume, *Haematostaphis* Hook. f., *Harpephyllum* Bernh., *Nothopegia* Blume, *Ozoroa* Delile, *Pachycormus* Coville ex Standl. or *Semecarpus* L. f. They all differ slightly from this fossil in the presence of taller upright marginal ray cells, thinner rays, or abundant septate fibers. These differences are not significant enough to dismiss a potential affinity with Anacardiaceae.

Most of the fossil wood specimens of Moraceae are affiliated with either the extant genus *Ficus* L. or the fossil genus *Ficoxylon* Kaiser (Gregory et al., 2009). Both commonly have larger rays than in our fossil and banded parenchyma and sometimes weakly differentiated sheath cells (Kaiser, 1880; Schenk, 1883, Koek-Noonnan et al., 1984b). Laticifers are absent in the fossil woods of *Antiaris*, *Cudranioxylon* Dupéron-Laudoueneix, *Moroxylon* Selmeier,

FIGURE 5 Wood type 1-b (Moraceae, Anarcardiaceae?, Kirkiaceae?). (A–C) MNHN.F.50229.2, transverse sections; (D–I, M) MNHN.F.50229.4, tangential longitudinal sections; (J–L) MNHN.F.50229.5, radial longitudinal sections. (A) Wood diffuse-porous, vessels solitary and in multiples (arrowhead). (B, C) Detail of vessels, often filled with orange material and surrounded by vasicentric parenchyma (arrowhead). (D) Fusiform 1–5-(6-)seriate rays and tyloses in vessel. (E) Detail of 4-seriate ray showing intercellular spaces (arrowhead). (F) Large, non-vestured intervessel pits. (G) Vasicentric axial parenchyma. (H) Parenchyma strand with at least up to five cells (arrowheads). (I) Parenchyma cells subdivided (arrowheads). (J) Heterocellular ray with body of procumbent cells and one marginal row of square/upright cells; numerous simple pits between ray parenchyma cells are visible (arrowhead). (K) Group of narrow vessels with simple perforation plates, apparently simple vessel-ray parenchyma pits (white arrowheads), intervessel pits (black arrowhead), and simple vessel-axial parenchyma pits (grey arrowhead). (L) Simple vessel-ray parenchyma pits (white arrowheads) and simple vessel-axial parenchyma pits (grey arrowhead). (M) Small branch trace. Scale bars: (A) 1 mm; (M) 500 μm; (B–D) 200 μm; (G, H, J) 100 μm; (E, I, K, L) 50 μm; (F) 25 μm.

Aginoxylon Dupéron, *Soroceaxylon* Franco, *Milicioxylon* Shukla, Mehrotra & Guleria (Dupéron, 1975; Dupéron-Laudoueneix, 1980; Awasthi, 1989; Selmeier, 1993; Franco, 2010; Shukla et al., 2013), *Maclura* (Martínez-Cabrera and Cevallos-Ferriz, 2006). Markedly radially longer than tall procumbent ray cells with many small punctuations are reported in *Crudanioxylon* (Dupéron-Laudoueneix, 1980) and in some extant genera (e.g., *Antiaris*, *Castilla* Cerv., *Perebea* Aubl., *Maquira* Aubl; Koek-Noonnan et al., 1984a). Fossil Moraceae woods differ from our fossil either because of ring-porous wood, common laticifers, distinct sheath cells, different vessel-ray pits, larger or thinner rays, more abundant axial parenchyma and wider vessels. It is difficult to assign our fossil to any existing genus, and it seems unwarranted to create a new one because many important diagnostic features are poorly visible in this fossil (the vessel diameter, the abundance of axial parenchyma and its arrangement, the presence of laticifers or septate fibers) or are variable (vessel density and diameter).

Among Anacardiaceae that have rays >3-seriate and no radial canals, the ones that most resemble the present fossil are *Dracontomeloxylon* Prakash, but species in that genus have a lower vessel density and wider vessels (Prakash, 1979), and *Coahuiloxylon* Estrada-Ruiz, Martínez-Cabrera & Cevallos-Ferriz differs in having smaller intervessel pits and a lower vessel density (Estrada-Ruiz et al., 2010).

Wood-type 1-c (Figure 6)

Affinity—Sapindales?

Material—MNHN.F.50230.1 to MNHN.F.50230.6 (field number of original specimen: PPP2)

Repository—Slides: plant fossil collection of the MNHN, Paris. Remains of original specimen: pending restitution to the collection of the Department of Geology at the University of Yangon (Myanmar)

Locality—Ngape Township, Minbu District, Magway Region, Myanmar

Age and stratigraphic position—Mid-Paleocene (Danian-Selandian), 61.3 ± 1.6 Ma, Paunggyi Formation

Description—Wood diffuse-porous. Growth ring boundaries absent. Vessels hardly visible due to compression. Few counted ($N = 36$) but they seem to be solitary (about 80%), and in pairs; round to oval in outline (Figure 6A), about 3–8/mm² (mean 4/mm²), tangential diameter 35–190 μm (mean 104 μm), radial diameter 90–185 μm (mean 126 μm). Tyloses not observed. Vessel element lengths 125–280 μm (mean 189 μm) long. Perforations simple (Figure 6E). Intervessel pits alternate, non-vestured, borders not visible, aperture oval, 3–6 μm (mean 4.5 μm) wide (Figure 6F). Vessel-ray parenchyma pits not visible; large pits with reduced borders to almost simple could be vessel-axial parenchyma pits (Figure 6I). Axial parenchyma arrangement difficult to determine, appears rare, 60–85 μm (mean 77 μm, $N = 5$) long, 18–24 μm (mean 20 μm, $N = 6$) wide; Figure 6D, G). Rays 1–4-seriate, mostly 2–3-seriate (1-seriate: 18%, 2-seriate: 42%, 3-seriate: 40%,

4-seriate: 10%), 5–12/mm (mean 8/mm), ray height 200–800 μm (mean 370 μm) or 6–41 cells (mean 19 cells) (Figure 6B), possibly up to 76 cells; multiseriate rays are heterocellular with body composed of procumbent cells with at least 1–3 marginal rows of square or upright cells (Figure 6H), uniseriate rays have mixed square, upright and procumbent cells. Kribs's ray type heterogeneous IIB. Sheath cells absent. Fibers apparently non-septate, arranged in radial rows (Figure 6A), 7–23 in tangential diameter (mean 15 μm). No mineral inclusion seen.

Estimated minimal diameter—Imprecise due to poor preservation, between 5–16.5 cm (more likely 12–16.5 cm)

Description in InsideWood codes (fossil code in parentheses)—2 5 13 22 25 42 46? 47? 52 75? 76? 79? 97 98v 106 107 115 168 (302 303v 313 315)

Affinities and remarks

This specimen does not show any distinctive diagnostic features. We searched the InsideWood database (2004 onward) using the following features: diffuse-porous wood with simple perforation plates (5p, 13p, 14a), alternate non-vestured intervessel pits (IVP) (20a, 22p, 29a), absence of large IVP (27a), vessels between 100–200 μm in tangential diameter and fewer than 20/mm² (40a, 42p, 48a, 49a, 50a), short vessel elements (52p), 1–3-seriate rays not of two sizes (96a, 97p, 99a, 103a), rays commonly with 1–4 marginal cells (105a, 106p, 107p, 115p), absence of storied rays (118a) and radial canals (130a). This combination of features occurs in 18 families. Among them, the taxa with the closest anatomy are found in Anacardiaceae, Burseraceae, Cannabaceae, Clusiaceae, Rutaceae, and Sapotaceae. However, Anacardiaceae and Burseraceae usually have wider intervessel pitting (>7 μm), few uniseriate rays and sometimes radial canals; Burseraceae have septate fibers; Cannabaceae generally have obvious paratracheal parenchyma and wider rays (mostly over 4-seriate); Clusiaceae often have higher rays (>1 mm); Rutaceae often have homocellular rays with few uniseriate ones and vessels in radial multiples are common; Sapotaceae have frequent tyloses and markedly heterocellular rays (Metcalfe and Chalk, 1950; InsideWood, 2004 onward). Many important features such as the presence or absence of septate fibers, the axial parenchyma distribution, the original density and diameter of vessels, and vessel-ray parenchyma pits cannot be accurately discerned in our fossil. Our observations indicate possible affinities with some taxa from the orders Ericales (Sapotaceae), Malpighiales (Clusiaceae), Rosales (Cannabaceae) or Sapindales (Anacardiaceae, Burseraceae, Rutaceae), but it is impossible to be more conclusive.

This specimen differs from Wood-type 1-a because of the apparent scarcity of the parenchyma, 2–3-seriate rays (against mostly 3–4-seriate) and the shape of the rays being less fusiform. It more resembles Wood-type 1-b regarding its ray composition (Figure 6C). But rays of this specimen are narrower on average than Wood-type 1-b, and the procumbent cells are less elongated. In addition, intervessel pits seems smaller in this specimen, although only the aperture is visible. This comparison is speculative because vessel-parenchyma pits could not be observed.
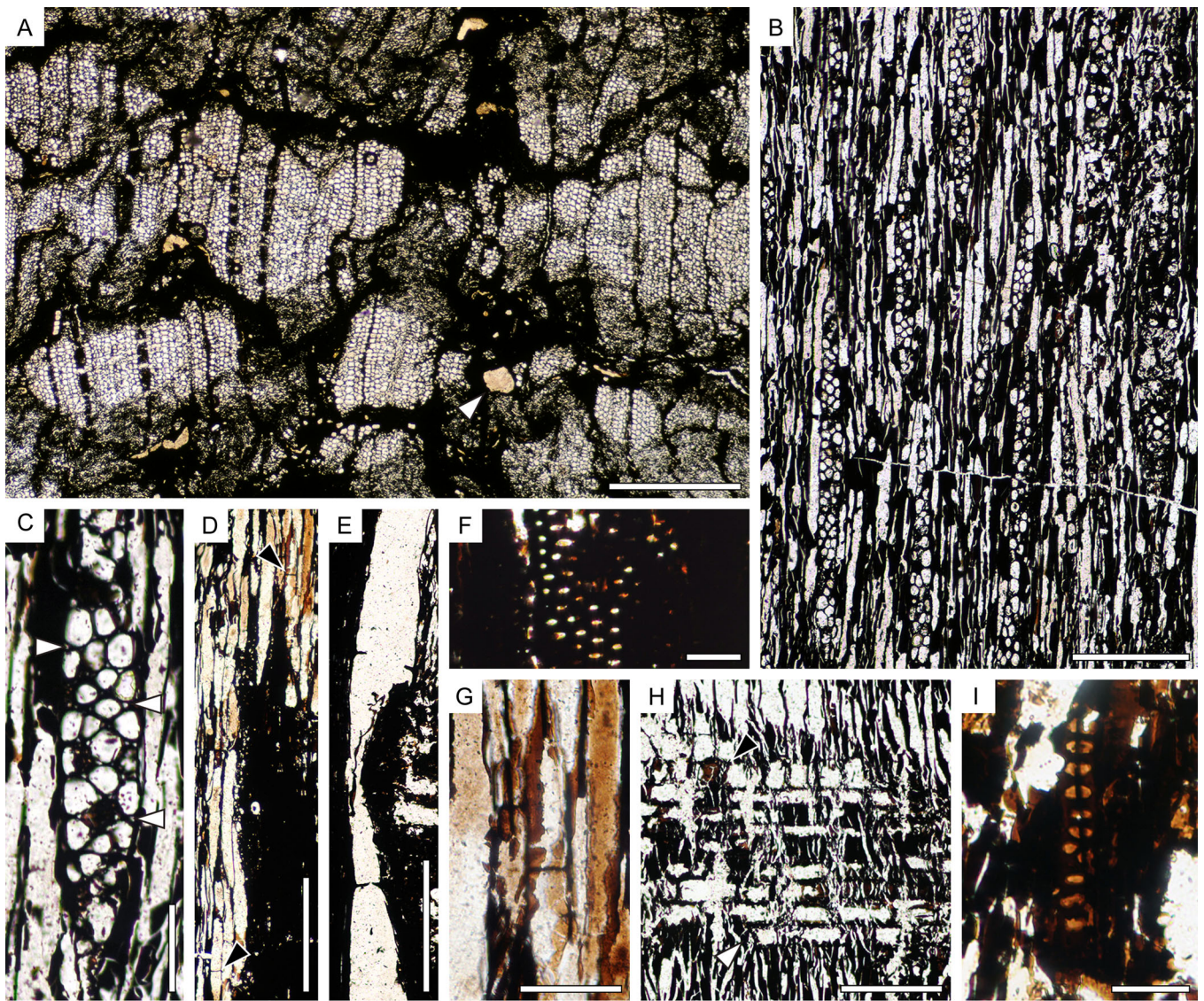
FIGURE 6 Wood-type 1-c (Sapindales?). (A) MNHN.F.50230.1, transverse section; (B–D, F–G, I) MNHN.F.50230.3, tangential longitudinal sections; (E, H) MNHN.F.50230.5, radial longitudinal sections. (A) Poorly preserved wood with some round and mostly solitary vessel poorly preserved (arrowhead). (B) Rays (1–4-seriate). (C) Detail of ray displaying intercellular spaces (arrowheads). (D) Vasicentric parenchyma marked by rare end walls (arrowheads). (E) Simple perforation plates. (F) Non-vestured intervessel pits. (G) Detail of parenchyma cells in upper corner of (C). (H) Heterocellular ray with procumbent cells (white arrowhead) and 1–3 marginal rows of square/upright cells (black arrowhead). (I) Likely vessel-axial parenchyma pits, with reduced borders to apparently simple. Scale bars: (A) 500 µm; (B, D) 200 µm; (E, H) 100 µm; (C, G) 50 µm; (F, I) 25 µm.

Wood-type 1-d (Figure 7)

Affinity—Laurales? (Lauraceae?)

Material—MNHN.F.50231.1 to MNHN.F.50231.7 (field number of original specimen: PPP6)

Repository—Slides: plant fossil collection of the MNHN, Paris. Remains of original specimen: pending restitution to the collection of the Department of Geology at the University of Yangon (Myanmar)

Locality—Ngape Township, Minbu District, Magway Region, Myanmar

Age and stratigraphic position—Mid-Paleocene (Danian-Selandian), 61.3 ± 1.6 Ma, Paunggyi Formation

Description—Wood diffuse-porous. No distinct growth-ring boundaries observed. Vessels mostly solitary (90%) and in radial multiples of 2–3 (10%) (Figure 7A); non-compressed vessels round in outline (Figure 7C), 5–11/mm² (mean 8/mm²), vessel tangential diameter 45–170 µm (mean 87 µm), minimum and mean likely underestimated due to compression, radial diameter 50–175 µm (mean 111 µm). Tyloses absent. Vessel element length 85–335 µm (mean 195 µm). Perforation plates simple. Intervessel pits alternate, non-vestured, 7–11.5 µm (mean 9.2 µm) wide, with large oval apertures (Figure 7D, E). Borders appear smaller close to perforations. Pits that could be vessel-ray parenchyma or vessel-axial parenchyma pits appear to be simple or with reduced borders (Figure 7K). Axial parenchyma only visible in longitudinal sections, paratracheal (probably scanty paratracheal to vasicentric) (Figure 7I), maybe also apotracheal, at
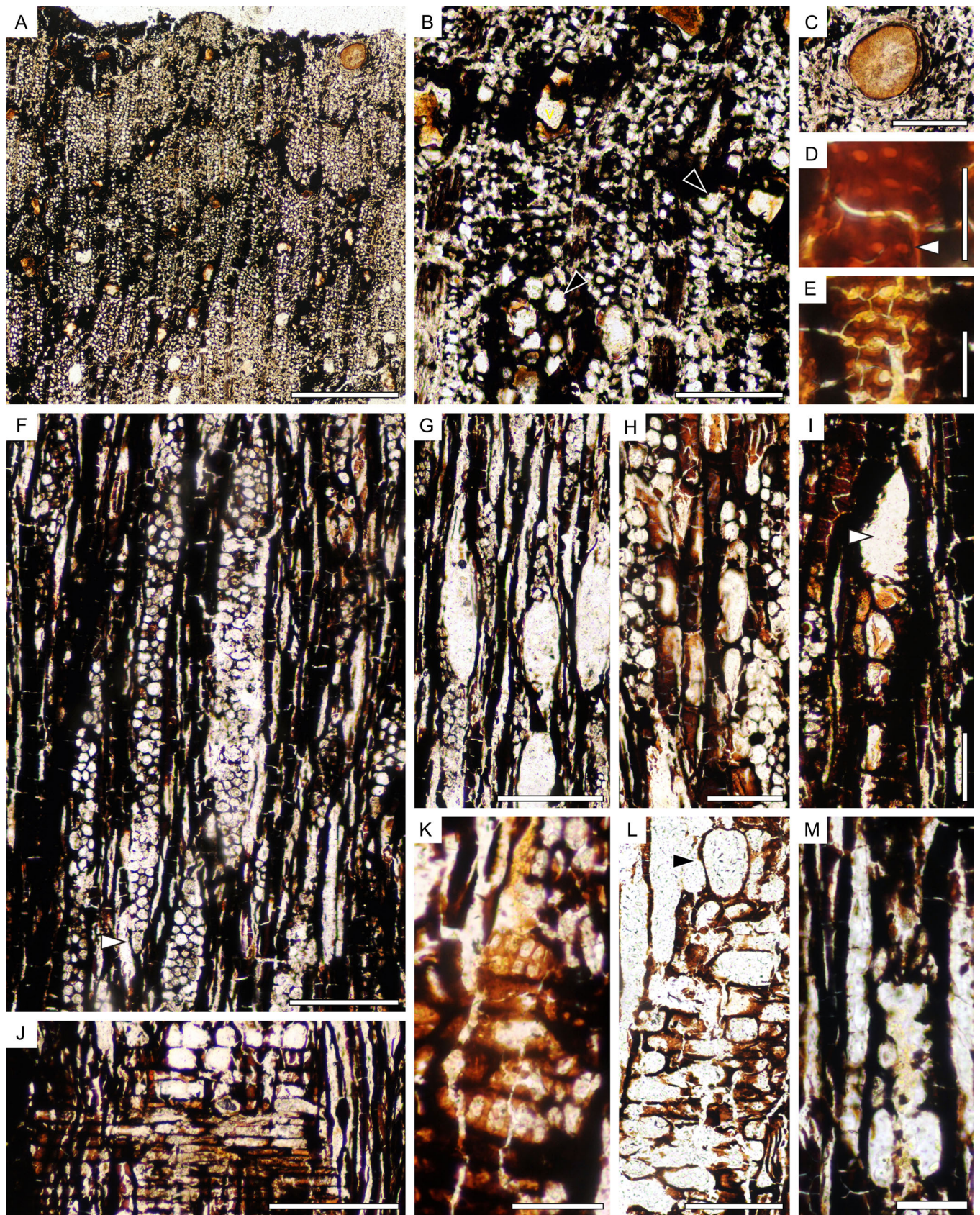
FIGURE 7   (See caption on next page).

least up to 4 cells per strand (Figure 7H). Parenchyma cells 55–180 μm (mean 94 μm) long and 17–39 μm (mean 27 μm) wide. Parenchyma strands sometimes look subdivided (Figure 7M), but this could be an artifact due to degradation. Rays 1–5-seriate, mostly 2–4-seriate (1-seriate: 5%, 2-seriate: 30%, 3-seriate: 39%, 4-seriate: 23%, 5-seriate: 3%), 4–11/mm (mean 7/mm), ray height 100–1530 μm (mean 470 μm) or 4–60 cells (mean 21 cells) (Figure 7F); some rays with end-to-end connections; heterocellular with procumbent body cells with 1–2 (maybe more) marginal rows of square to upright cells (Figure 7J, L), with a possible tendency for ray cell types to be intermixed in the rays. Kribs's ray type heterogeneous IIB. Sheath cells absent. Fibers arranged in radial rows, 16–31 μm in tangential diameter (mean 23 μm). Lacunae, possibly idioblasts (oil cells) or evidence of decay, visible in tangential section (Figure 7G). Some cells in transverse section (Figure 7B, arrowhead) could represent these possible oil cells or axial parenchyma cells.

Estimated minimal diameter—between 5 and 8 cm

Description in InsideWood codes (fossil code in parentheses)—5 9 13 22 26 27v 30? 31? 32? 41? 42? 47 52 65? 66 78 79 80? 92 93? 97 98 102v 106 107v 115 136 142 168 (300? 302 308 313 315)

Affinities and remarks—

In this wood, it is difficult to ascertain some important diagnostic features, such as the axial parenchyma arrangement, type of vessel-ray parenchyma pits, presence of crystals and septate fibers. The combined features of the specimen are not found in any extant species in the InsideWood (2004 onward) database. We searched the InsideWood database (following the spreadsheet method mentioned in Materials and Methods) using the following features: diffuse-porous wood (5p), exclusively simple perforation plates (13p, 14a), alternate, non-vestured pitting that is not minute, at least medium (22p, 24a, 26p, 29a), vessel diameter, neither narrow or wide (40a, 43a) between 5 and 40 vessels/mm² (46a, 49a, 50a), paratracheal parenchyma (78p and/or 79p and/or 80p), 1–3- and 4–10-seriate rays (96a, 97p, 98p, 99a, 100a), heterocellular rays (104a, 105a), 2 or more cells per axial parenchyma strand (90a), and excluding rare or absent parenchyma (75a), sheath cells (110a or 110v), storied rays (118a) and radial canals (130a or 130v). The database yielded seven families with these features: Anacardiaceae, Cannabaceae, Lauraceae, Moraceae, Phyllanthaceae, Rhamnaceae, Meliaceae.

The enlarged marginal ray cells (Figure 7L) could be oil cells or crystalliferous idioblasts. In tangential sections, large lacunae are sometimes observed (Figure 7G) and could be a result of wood decay or represent large oil cells (yellowish droplets in these shapes could be oil). The presence of oil cells would indicate that this wood is a Lauraceae, close to the genus *Beilschmiedia* Nees, a genus that has vasicentric parenchyma, few oil cells among fibers, and few septate fibers. *Actinodaphne* Nees, *Aspidostemon* Rohwer & H.G.Richt. and some *Ocotea* Aubl. share some similarities, especially regarding the parenchyma arrangement, the few oil cells sometimes among fibers, and the size of rays or the diameter of vessels for some species. The oil cells found in *Aniba rosodora* Ducke, *Licaria triandra* (Sw.) Kosterm. or *Persea borbonia* (L.) Spreng., either among fibers or among rays (Figure 7L), also look similar to those of the present fossil. But these three species have rays rarely over 3-seriate and numerous septa in fibers (InsideWood, 2004 onward). Lauraceae often have tyloses, longer vessel elements, and sometimes septate fibers (Metcalfe and Chalk, 1950; InsideWood, 2004 onward). Anacardiaceae have mostly rays narrower than 3-seriate and crystals in rays. Cannabaceae have mostly wider rays, often confluent parenchyma and crystals in ray cells. Phyllanthaceae are very variable with tall, numerous, and very heterocellular rays. Rhamnaceae often display distinct growth rings (although maybe not near the equator in the Paleocene), smaller intervessel pits and bordered vessel-ray parenchyma pits. Meliaceae are dismissed by their small intervessel pits. This specimen resembles Wood-type 1-b (affinity with Moraceae) but is less well preserved. Both have scanty paratracheal to vasicentric parenchyma, large and non-polygonal intervessel pits, same general vessel disposition, well-defined procumbent ray parenchyma cells (see affinities and remarks for Wood-type 1-b), and no laticifers. However, it has taller rays, no tyloses, no clear vessel-ray parenchyma pits, more abundant axial parenchyma and narrower and fewer vessels. These differences could be due to anatomical variation and poor preservation. Indeed, in fossil Wood-type 1-b, some very sporadic lacunae are visible, but they are likely a preservation artifact. Thus, this specimen appears to be closer to Lauraceae than the other families mentioned above, although they are not totally dismissed, especially Moraceae, which is the best affinity for Wood-type 1-b.

FIGURE 7 Wood-type 1-d (Lauraceae?). (A–C) MNHN.F.50231.1, transverse sections; (D–H, M) MNHN.F.50231.3, tangential longitudinal sections; (I–L) MNHN.F.50231.6, radial longitudinal sections. (A) Diffuse-porous wood with mostly solitary vessels, presence of small pores that could be large fibers, axial parenchyma cells, small vessels or oil cells. (B) Small vessels with likely axial parenchyma or oil cells around them (arrowheads). (C) Detail of round and non-compressed vessel surrounded by vasicentric (to aliform?) parenchyma. (D, E) Large, non-vestured intervessel pits (arrowhead). (F) Rays (1–5-seriate) with cells of different size, square or upright marginal cell (black arrowhead). (G) Lacunae either due to wood decay or possible large oil cells; the surrounding rays and fibers seem to follow the shape of the lacunae. (H) Parenchyma with at least 4 cells per strand. (I) Vasicentric parenchyma around a vessel (arrowhead). (J) Heterocellular ray with procumbent body cells and 1–2 marginal rows of square or upright cells. (K) Possible simple vessel-ray pits. (L) Ray with one enlarged upright marginal cell (originally containing crystal?/small oil cell?). (M) Possibly subdivided parenchyma strand with half of a degraded ray on the right. Scale bars: (A, F) 500 μm; (B, C, G, J) 200 μm; (D, E) 25 μm; (H, I, L) 100 μm; (K, M) 50 μm.

The genus *Ubiquitoxylon* Wheeler was instituted for fossil woods with a combination of features that occurs in multiple families, including the Anacardiaceae and Lauraceae. Wood-type 1-d shares most of the features of this genus, including the occurrence of enlarged marginal ray cells, but it does not have idioblasts amongst the fibers and axial parenchyma is rare to scanty paratracheal (Wheeler et al., 2019). However, given the poor state of preservation of sample MNHN.F.50231 (PPP6), it seems unwise to assign it to a genus.

Group 2: Uni-biseriate rays

Wood-type 2-a (Figure 8)
Affinity—Sapindales (Anacardiaceae)
Material—MNHN.F.50232.1 to MNHN.F.50232.6 (field number of original specimen: PPP5)
Repository—Slides: plant fossil collection of the MNHN, Paris. Remains of original specimen: pending restitution to the collection of the Department of Geology at the University of Yangon (Myanmar)
Locality—Ngape Township, Minbu District, Magway Region, Myanmar
Age and stratigraphic position—Mid-Paleocene (Danian-Selandian), 61.3 ± 1.6 Ma, Paunggyi Formation
Description—Wood diffuse-porous. No growth ring boundaries visible. Vessels mainly solitary (about 70–82%) or in radial multiples of 2–3 (rarely 4) (18–30%) (Figure 8A); solitary vessels probably round to oval in outline (Figure 8B), 3–9/mm² (mean 6/mm²), tangential diameter 50–225 μm (mean 155 μm), radial diameter of the less compressed vessels 87–160 μm (mean 122 μm). Tyloses present (Figure 8B, F). Vessel element length (115) 190–445 μm (mean 260 μm). Perforation simple (Figure 8I). Intervessel pits alternate, non-vestured, 5.8–13.5 μm (mean 9 μm) wide with a large lenticular aperture (Figure 8G). Vessel-ray parenchyma pits mostly of the same size as intervessel pits, sometimes elongated, with reduced borders to apparently simple, 2–9 per ray cell (Figure 8I). Vessel-axial parenchyma pits apparently the same as vessel-ray parenchyma pits. Axial parenchyma appears to be scanty paratracheal to vasicentric (Figure 8B), tangential sections show axial parenchyma strands adjacent to vessels, with up to 4 cells per strand (Figure 8E). Parenchyma cells 50–175 μm (mean 100 μm) long and 20–35 μm (mean 27 μm) wide in tangential section. Rays 1–2-(3-)seriate, (1-seriate: 60–72%, 2-seriate: 27–39%, 3-seriate: 1%), rays often uniseriate for most of their height, with a small biseriate part 1–2 cells high, 4–9/mm (mean 6/mm), ray height (105) 130–600 μm (mean 260 μm) or 4–26 cells (mean 10 cells) (Figure 8D); ray heterocellular with a variable composition, multiseriate rays with procumbent (to almost square) body cells with 1–4 marginal rows of square or upright cells Figure 8H), uniseriate rays tend to be composed of square and upright cells. Kribs's ray type heterogeneous III to IIA. Sheath cells absent. Fibers probably non-septate, poorly

preserved, arranged in radial rows, 12–28 μm in tangential diameter (mean 20 μm). No mineral inclusions. Two smalls branch traces present (Figure 8J). Helical thickenings present in the elements of the branch traces, likely primary xylem (Figure 8C).

Estimated minimal diameter—Difficult to estimate due to poor preservation, between 3 and 7 cm, (more likely 4 cm)

Description in InsideWood codes (fossil code in parentheses)—2 5 13 22 25 26 27 31 42 47 52 56 66 78? 79? 92 97 106v 107v 108v 109v 115 168 (300 302 313 315)

Affinities and remarks

Diffuse-porous wood (5p), with simple perforation plates (13p), intervessel pits large, non-vestured and alternate (22p, 24a, 27p, 29a), vessel-ray pits with reduced borders to apparently simple (31p), tyloses (56p), vasicentric parenchyma (79p), short rays uni- and biseriate (97p, 98a, 99a, 102a), heterocellular (104a, 105a) strongly recall Anacardiaceae and Burseraceae (InsideWood, 2004 onward). Other families including Lauraceae, Cannabaceae and some Bonnetiaceae, or Euphorbiaceae share similar features. Burseraceae always have septate fibers, only rare or scanty paratracheal parenchyma, sometimes radial canals, often crystals in ray cells (Metcalfe and Chalk, 1950; InsideWood, 2004 onward) and always large intervessel pits (>8 μm; Pace et al., 2022). Anacardiaceae are very similar to Burseraceae with few differences such as less frequent tyloses, septate and non-septate fibers, sometimes shorter vessel elements, parenchyma mostly scanty paratracheal and vasicentric, as well as sometimes more developed in aliform, confluent and banded; they can have many rows of marginal ray cells (Metcalfe and Chalk, 1950; InsideWood, 2004 onward) and intervessel pits <8 μm (Pace et al., 2022). The absence of septate fibers and the presence of vasicentric parenchyma in our specimen thus suggest a more likely affinity to Anacardiaceae and to the *Mangifera-Gluta-Anacardium* group, which has rare radial canals, frequent uniseriate rays, few or no septate fibers, and tyloses common (Metcalfe and Chalk, 1950; InsideWood, 2004 onward). This group includes *Fegimanra* Pierre, *Anacardium* L., *Bouea* Meisn., *Mangifera* L., *Swintonia* Griff, *Gluta* L. (Weeks et al., 2014; Muellner-Riehl et al., 2016). However, *Gluta* often have banded parenchyma and some radial canals (InsideWood, 2004 onward). The preservation state of our specimen does not allow a more precise identification.

The fossil record of wood related to Anacardiaceae is large (Gregory et al., 2009): Estrada-Ruiz et al. (2010) counted more than 75 published fossils. The specimens with 1–3-seriate rays and mostly vasicentric parenchyma are described under the genera *Anacardioxylon* Felix, *Bouea*, *Buchananioxylon* Ghosh & Roy, *Holigarnoxylon* Prakash & Awasthi, *Glutoxylon* (Chowdhury) Prakash & Tripathi, *Mangiferoxylon* Awasthi, *Tapirira* Aubl. and *Llanodelacruzoxylon* Rodríguez-Reyes, Estrada-Ruiz & Gasson. This specimen is most similar to *Anacardioxylon* and *Mangiferoxylon*. The other genera differ in having either radial

FIGURE 8 (See caption on next page).

canals, diffuse or aliform-confluent to banded parenchyma (Gupta, 1935; Chowdhury, 1936; Prakash and Awasthi, 1970; Bande and Prakash, 1984; Agarwal, 1988; Srivastava and Saxena, 1998; Wheeler and Manchester, 2002; Rodríguez-Reyes et al., 2020). *Mangiferoxylon* has mostly 1–2-seriate rays, non-septate fibers but also aliform to confluent and terminal parenchyma, and frequent crystals in ray cells (Awasthi, 1966). Many fossils are described as *Anacardioxylon*; they mostly have narrow vasicentric parenchyma, 1–2-seriate rays, which are heterocellular with 1–3 rows or marginal cells, and vessels mostly solitary. The remaining features are more heterogeneous between specimens (Schönfeld, 1947; Prakash and Dayal, 1965; Awasthi, 1974; Prakash and Tripathi, 1976; Lemoigne, 1978; Crawley, 2001). Nonetheless, our fossil cannot be attributed to these genera with any confidence because some diagnostic features are poorly preserved (septa, arrangement of the parenchyma, growth rings boundaries, terminal parenchyma, and crystal occurrences).

Wood-type 2-b (Figure 9)

Affinity—Sapindales or Myrtales? (Combretaceae?)

Material—MNHN.F.50233.1 to MNHN.F.50233.8 (field number of original specimen: PPP7), sample compressed

Repository—Slides: plant fossil collection of the MNHN, Paris. Remains of original specimen: pending restitution to the collection of the Department of Geology at the University of Yangon (Myanmar)

Locality—Ngape Township, Minbu District, Magway Region, Myanmar

Age and stratigraphic position—Mid-Paleocene (Danian-Selandian), 61.3 ± 1.6 Ma, Paunggyi Formation

Description—Wood diffuse-porous. No growth-ring boundaries visible. Vessels mainly solitary (95%, $N = 27$), likely originally oval in outline (Figure 9A), 4–6/mm², tangential diameter 22–94 μm (mean 58 μm) and radial diameter 70–220 μm (mean 140 μm; true diameter before compression being likely larger). Tyloses not observed. Vessel element length not measurable. Perforations seem simple. Intervessel pits alternate, non-vestured, 5.7–12.5 μm in horizontal diameter (mean 9.6 μm), with large oval lenticular apertures (Figure 9C). Vessel-ray parenchyma pits usually similar in size to intervessel pits, sometimes enlarged, but likely with reduced borders to apparently simple, with borders of variable size, 5–10.3 μm (mean 7.8 μm) large (Figure 8F–H). Axial parenchyma rarely observed, only visible in tangential section as scanty paratracheal (or vasicentric). Rays 1–2-seriate,

predominantly uniseriate (1-seriate: 92%, 2-seriate: 8%), 5–12/mm (mean 9/mm), ray height 87–720 μm (mean 246 μm) or 2–30 cells (mean 10 cells) (Figure 9B); heterocellular, made of procumbent body cells with 1 row of square or upright marginal cells (rarely 2–3 rows) (Figure 9D, E), sometimes a faint tendency for square and procumbent cells intermixed throughout the rays (Figure 9D); the shorter rays are probably only composed of square or upright cells. Kribs's ray type heterogeneous III. Fibers apparently non-septate, cell walls poorly defined, radially aligned, 8–24 μm in tangential diameter (mean 15.5 μm). Crystals maybe present in upright and procumbent ray cells (Figure 9B, D, E).

Estimated minimal diameter—Difficult to estimate due to bad preservation and compression, between 4 and 7 cm

Description in InsideWood codes (fossil code in parentheses)—2 5 9? 13 22 26 27 30 31v 41? 42? 46? 47? 66 78 96 106 115 136 137 138 168 (300v 302 307 313 315)

Affinities and remarks

This specimen is characterized by (1) diffuse-porous wood, (2) simple perforation plates, (3) large, non-vestured, alternate intervessel pits, (4) vessel-ray parenchyma pits with reduced borders to apparently simple, (5) scanty paratracheal or vasicentric parenchyma, (6) <30 cells high uniseriate rays, (7) heterocellular rays with mostly 1 row of upright marginal cells, (8) crystals in ray cells. This wood differs from Wood-type 2-a in having possibly bordered vessel-ray pits, almost exclusively uniseriate rays (compared to commonly 1–2-seriate), a greater ray density (up to 5–12/mm vs. 4–9/mm) and maybe crystals in ray cells. A search of InsideWood for diffuse-porous wood (5p) with exclusively simple perforation plates (13p, 14a), alternate, non-vestured intervessel pits not minute, at least medium (22p, 24a, 26p or 27p, 29a), heterocellular uniseriate rays (96p, 104a, 106p) and prismatic crystals (136p) gave several results, mostly species of Anacardiaceae, Burseraceae, Combretaceae, and Sapindaceae and a few Euphorbiaceae and Rhamnaceae. Only few species among Anacardiaceae and Burseraceae have exclusively uniseriate rays (10–16% according to InsideWood, 2004 onward). Both families frequently have radial canals (about half of the taxa; InsideWood, 2004 onward) and vessel-ray parenchyma pits always with reduced borders to apparently simple. The vessel-ray parenchyma pits of our fossil seem to have reduced borders (Figure 9G, H); even some simple pits are visible (Figure 9F). Among Combretaceae, only some *Terminalia* L. species have non-vestured pits (Inside-Wood, 2004 onward), but their parenchyma is mostly aliform, and rays can be very numerous. Euphorbiaceae,

---

FIGURE 8 Wood-type 2-a (Anacardiaceae). (A, B) MNHN.F.50232.1, transverse sections; (D, E, J) MNHN.F.50232.3, tangential longitudinal sections; (C, F–I) MNHN.F.50232.5, radial longitudinal sections. (A) Vessel solitary (arrowhead) or in short radial multiples. (B) Solitary vessel surrounded by vasicentric parenchyma (or scanty paratracheal) (white arrowhead), tyloses in vessel (black arrowhead). (C) Helical thickening in the small elements of a branch trace, probably primary xylem (arrowhead). (D) Rays (1–2-seriate). (E) Paratracheal axial parenchyma associated with vessel with up to 4 cells per strand. (F) Vessel plugged with tyloses. (G) Non-vestured intervessel pits. (H) Heterocellular ray with procumbent body cells (black arrowhead) and 1–4 marginal rows of square or upright cells (white arrowhead). (I) Simple perforation plate and crowded simple vessel-ray pits. (J) One of the two small branch traces. Scale bars: (A, J) 500 μm; (B, D) 200 μm; (C, E, F, H) 100 μm; (G, I) 50 μm.
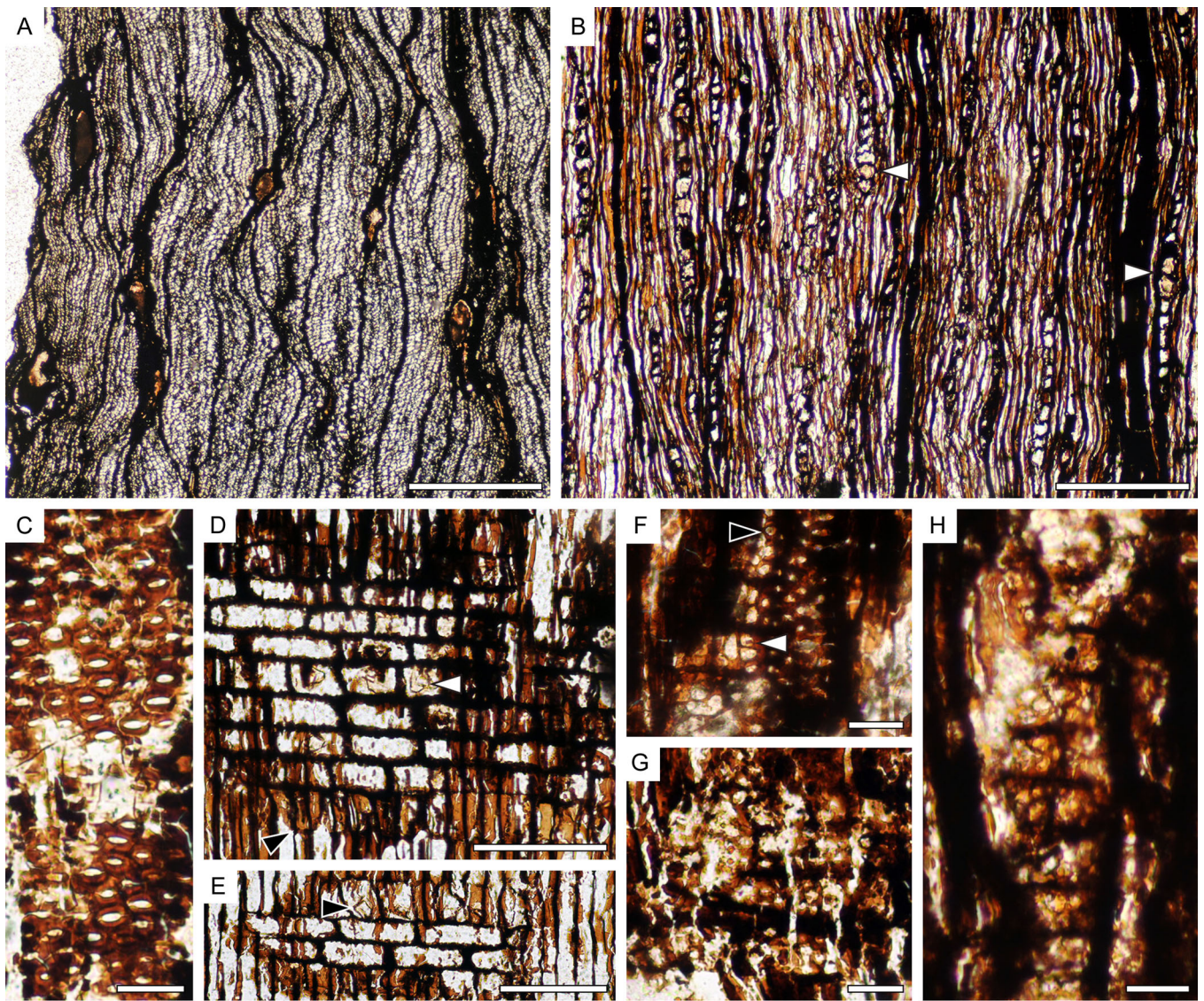
FIGURE 9 Wood-type 2-b (Sapindales, Combretaceae?). (A) MNHN.F.50233.1, transverse section; (B) MNHN.F.50233.3, tangential longitudinal sections; (C–H), MNHN.F.50233.6, radial longitudinal sections. (A) Poorly preserved and laterally compressed vessels. (B) Uniseriate rays with some cells probably containing crystals (arrowheads), non-septate fibers. (C) Large non-vestured intervessel pits. (D) Heterocellular ray with 1 marginal row of upright cells (black arrowhead), likely crystals in procumbent to almost square ray cells (white arrowhead). (E) Crystal in upright marginal ray cell (arrowhead). (F) Intervessel pits (black arrowhead), possible simple vessel-ray pits (white arrowhead). (G, H) Other possible vessel-ray parenchyma pits but seemingly with more or less reduced borders. Scale bars: (A) 500 μm; (B) 200 μm; (C, F–H) 25 μm; (D, E) 100 μm.

mostly have very heterocellular and numerous rays, frequently over 1 mm high, and axial parenchyma is mostly apotracheal (InsideWood, 2004 onward). Rhamnaceae mostly have multiseriate rays except for *Ziziphus* Mill. Sapindaceae often have marginal parenchyma, intervessel pits mostly small, never large, rays often uniseriate sometimes heterocellular, vessel-ray pits similar to intervessel pits and crystals more frequent in parenchyma than rays (Metcalfe and Chalk, 1950; InsideWood, 2004 onward).

Fossil woods sharing the diagnostic features of the specimen are also found in Anacardiaceae, Burseraceae, Combretaceae, Ebenaceae, and Euphorbiaceae. The main differences between this fossil and the Anacardiaceae are that the rays of the Anacardiaceae are generally not exclusively uniseriate, axial parenchyma is more common, and radial canals are common. The differences with Burseraceae are that they always have septate fibers, mostly multiseriate rays, and often radial canals. One fossil of Burseraceae has dominantly uniseriate rays and very sparse parenchyma: *Tetragastroxylon* Martínez-Cabrera, Cevallos-Ferriz & Poole. The differences from *Tetragastroxylon* are very large vessels (>200 μm) and some wide rays containing canals (Martínez-Cabrera et al., 2006). Among Combretaceae, the genus *Terminalioxylon* has mostly uniseriate rays, septate or non-septate fibers, parenchyma ranging from scanty paratracheal to confluent-banded. The main

differences are vestured intervessel pits and rays weakly heterocellular with crystals in enlarged or upright cells in the middle of procumbent cells (Mädel-Angeliewa and Müller-Stoll, [1973]). The preservation state of our fossil makes some features hard to determine, so it is difficult to be more conclusive; an affinity with Sapindales or less likely with Combretaceae, (both in Malvids) is thus only suggested.

Wood-type 2-c (Figure 10)

Affinity—Sapindales? (Anacardiaceae?)

Material—MNHN.F.50234.1 to MNHN.F.50234.6 (field number of original specimen: PPP8), poorly preserved

Repository—Slides: plant fossil collection of the MNHN, Paris. Remains of original specimen: pending restitution to the collection of the Department of Geology at the University of Yangon (Myanmar)

Locality—Ngape Township, Minbu District, Magway Region, Myanmar

Age and stratigraphic position—Mid-Paleocene (Danian-Selandian), 61.3 ± 1.6 Ma, Paunggyi Formation

Description—Wood diffuse-porous. Growth-ring boundaries indistinct. Vessels are solitary (85%) or in pairs (15%), solitary vessels round to oval in outline, 5–13/mm² (mean 6/mm²), tangential diameter 50–155 μm (mean 105 μm), radial diameter 70–120(150) μm (mean 100 μm) (Figure 10A, B). Vessel element length 185–535 μm (mean 305 μm). Perforations simple (Figure 10C). Intervessel pits alternate, non-vestured with oval apertures more or less elongated, 6–12 μm in horizontal diameter (mean 8.6 μm) (Figure 10C). Only a few vessel-ray parenchyma pits observed, likely with reduced borders (Figure 10G). Axial parenchyma barely visible in tangential or radial sections as scanty paratracheal or vasicentric (Figure 10D). Axial parenchyma cells poorly preserved, 60–100 μm (mean 78 μm) long and 18–30 μm (mean 24 μm) wide (Figure 10E). Rays 1–2(–3-)seriate, (1-seriate: 76%, 2-seriate: 21%, 3-seriate: 3%), 2–7/mm (mean 4/mm), ray height (90)123–475 μm (mean 240 μm) or 3–17 cells (mean 9 cells) (Figure 10D, F); heterocellular made of procumbent body cells (sometimes almost square) with 1–3 marginal rows of square or upright cells (Figure F, H, I). Kribs's ray type heterogeneous III to IIA or IIB. Fibers seemingly non-septate (Figure 10F), radially and often tangentially aligned, 13–31 in tangential diameter (mean 21 μm).

Estimated minimal diameter—between 5 and 7 cm

Description in InsideWood codes (fossil code in parentheses)—2 5 13 22 26 27 31? 41? 42? 47 52 66 78 79 97 106 107 114v 115v 168 (300? 302 313 315)

Affinities and remarks

As for the other Group 2 specimens, this sample is characterized by (1) diffuse-porous wood, (2) simple perforation plates, (3) large, non-vestured, alternate intervessel pits, (4) scanty paratracheal or vasicentric parenchyma, (5) mostly short (≤30 cells high) 1–3-seriate rays, (6) heterocellular rays with 1–3 row of square or upright marginal cells. Although similar to Wood-type 2-a (in ray

size and composition, axial parenchyma type, tyloses, and vessels density), this specimen differs from the previous ones because of its narrow and more numerous vessels, and its shorter rays (up to 17 cells high vs. 26 and 30—although the average height is similar: 9–10 cells). It is possible that these differences are related to preservation factors or intraspecific variation. This fossil shares features with Anacardiaceae (InsideWood, [2004] onward), and particularly with the *Mangifera-Gluta-Anacardium* group, which frequently has heterocellular uniseriate rays, mostly vasicentric parenchyma, commonly non-septate fibers and large intervessel pits. Two rays in our fossil are remarkably larger than the others (over 4-seriate); they could be due to either the vicinity of radial canals (which are sometime present in Anacardiaceae) or a growth perturbation. Although the few observable vessel-ray pits seem to have a reduced border (Figure 10G), their nature is ambiguous. The intervessel pits themselves have sometimes barely visible borders, either by nature or because of degradation.

The affinities and remarks about the resemblance of Wood-type 2-a to previously published fossil woods of Anacardiaceae applies to this wood.

Wood-type 2-d (Figure 11)

Affinity—Incertae sedis

Material—MNHN.F.50235.1 to MNHN.F.50235.6 (field number of original specimen: PPP10)

Repository—Slides: plant fossil collection of the MNHN, Paris. Remains of original specimen: pending restitution to the collection of the Department of Geology at the University of Yangon (Myanmar)

Locality—Ngape Township, Minbu District, Magway Region, Myanmar

Age and stratigraphic position—Mid-Paleocene (Danian-Selandian), 61.3 ± 1.6 Ma, Paunggyi Formation

Description—Wood strongly compressed, almost all vessels are crushed (Figure 11A). Likely diffuse-porous. Growth-ring boundaries absent. Solitary vessels probably oval in outline (?), radial groups of 2 seen in radial section, 4–10/mm² (?), tangential diameter 63–76 μm (mean 70 μm, *N* = 7), radial diameter 60–170 μm (mean 110 μm, *N* = 15). Tyloses not observed, vessels sometimes filled with brown contents (Figure 11A). Vessel elements 142–320 μm (mean 225 μm, *N* = 10) long. Perforation simple. Intervessel pits only seen in radial section, alternate, with a lenticular aperture, non-vestured, 6–11.5 μm (mean 8.1 μm) large (Figure 11C). Vessel-ray parenchyma pits not clearly seen, either similar to intervessel pits (Figure 11I) or with a reduced border to apparently simple (Figure 11H), sometime enlarged, 6–13 μm (mean 9.9 μm) large. Vessel-axial parenchyma pits similar to intervessel pits although less crowded and sometimes enlarged (Figure 11G). Parenchyma vasicentric or scanty paratracheal, only visible in radial section (Figure 11G). Parenchyma cells 40–70 μm (mean 58 μm) long and 20–28 μm (mean 24 μm) wide. Rays 1–3-seriate, mostly 1–2-seriate (1-seriate: 41%, 2-seriate: 55%,
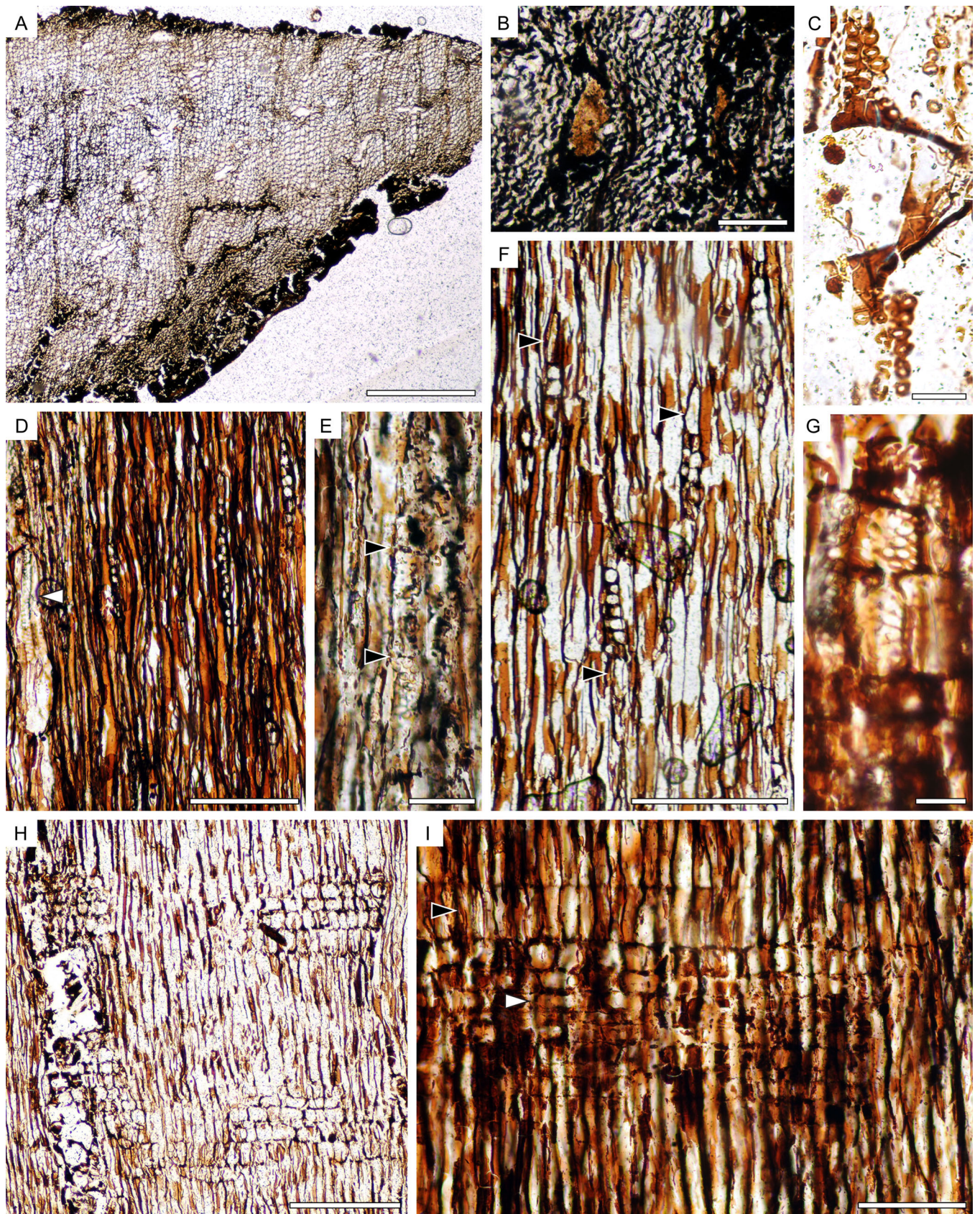
FIGURE 10 (See caption on next page).

3-seriate: 4%), 3–7/mm (mean 5/mm), ray height 63–450 µm (mean 215 µm) or 4–21 cells (mean 11 cells) (Figure 11D); heterocellular made of procumbent body cells with 1(–3) marginal rows of square or upright cells (Figure 11E, F), sometimes small uniseriate rays are composed only of square or upright cells. Kribs's ray type heterogeneous IIB (to IIA). Fibers non-septate, arranged in radial rows, 9–22 µm in tangential diameter (mean 16 µm). Crystals in (sometimes enlarged) ray cells, mostly the upright ones, 23–27 µm maximum diameter (Figure 11B, E, F).

Estimated minimal diameter—not possible to determine

Description in InsideWood codes (fossil code in parentheses)—2 5 13 22 26 27v 30? 31? 41? 42? 47? 52 66 78? 79 97 106 107v 115 136 137 156? 168 (300? 302 307 313 315)

Affinities and remarks

This specimen is very similar to the other Group 2 specimens: (1) diffuse-porous wood with simple perforation plates, (2) alternate, non-vestured intervessel pits, (3) thin rays mainly 1–2-seriate, less than 30 cells high, (4) heterocellular rays with 1–3 marginal rows of upright cells, (5) scanty paratracheal or vasicentric parenchyma. This combination of features, as for the previous specimens, recalls the Anacardiaceae (Burseraceae are dismissed because they always display septate fibers, which are not present in our fossil.). The presence of crystals in ray cells that sometimes appear enlarged (Figure 11F) is consistent with the family and can be seen, for instance, in *Astronium* Jacq. (InsideWood, 2004 onward). This feature is shared by Wood-type 2-b as is the presence of crystals in rays and possibly borders in vessel-ray parenchyma pits. However, this specimen differs from the other Group 2 specimens because of mostly 2-seriate rays. Vessel-ray pits seem to have reduced borders (Figure 11H), but because intervessel pits have a wide aperture with a narrow border, the distinction between both intervessel and vessel-parenchyma pits is not clear. Vessel-ray parenchyma pits may be bordered, similar to intervessel pits (Figure 11I), which would bring the fossil closer to the Rhamnaceae or Sapindaceae families (see Wood-type 2-b). Because some key features are ambiguous or not clearly visible, we cannot confidently assign this specimen to any taxon, but we do note a resemblance to the Anacardiaceae.

For comparison with fossil taxa, see the affinities and remarks for Wood-types 2-a and 2-b.

Group 3: Scalariform perforation

Affinity—Incertae sedis

Genus—*Compitoxylon* Gentis, De Franceschi et Boura gen. nov.

Type species—*Compitoxylon paleocenicum* Gentis, De Franceschi et Boura sp. nov.

Generic diagnosis—Wood diffuse-porous. Scalariform perforation plates. Intervessel pits alternate, non-vestured. Axial parenchyma diffuse to diffuse-in-aggregates. Rays uniseriate and multiseriate, >1 mm high, almost exclusively made of square and upright ray cells. Sheath cells present. Fibers non-septate.

Etymology—The name *Compitoxylon* comes from the Latin *compitum* for crossroad or intersection (referring to the anatomical features of the genus found in diverse, unrelated extant taxa) and the suffix -*xylon* used for fossil wood.

Compitoxylon paleocenicum Gentis, De Franceschi et Boura sp. nov. (Figure 12)

Specific diagnosis

Wood diffuse-porous, vessels solitary and in radial multiples, vessel diameter <150 µm, vessel density between 10–40/mm². Vessel element length >350 µm. Perforation plates exclusively scalariform with <20 bars. Intervessel pits alternate, non-vestured with round apertures. Parenchyma diffuse to diffuse-in-aggregates. Rays 1–7-seriate, up to 5 mm high and averaging >1 mm. Sheath cells present. Rays composed almost exclusively of square and upright cells. Fibers non-septate.

Holotype—Slides from MNHN.F.50236.1 to 50236.6 (field number of original specimen: PPP1)

Type locality—Ngape Township, Minbu District, Magway Region, Myanmar

Repository—Slides: plant fossil collection of the MNHN, Paris. Remains of original specimen: pending restitution to the collection of the Department of Geology at the University of Yangon (Myanmar)

Age and stratigraphic position—Mid-Paleocene (Danian-Selandian), 61.3 ± 1.6 Ma, Paunggyi Formation

Etymology—The epithet *paleocenicum* refers to the age of the Paunggyi Formation from which the fossil comes.

Description—Wood diffuse-porous. No clear growth-ring boundaries visible although the vessel density seems to vary (Figure 12A). Vessels solitary (45–80%) and in radial multiples of 2–7 (mostly 2–3) (20–55%) (Figure 12F), rarely in small clusters; solitary vessels round to oval, 13–35/mm²

FIGURE 10 Wood-type 2-c (Anacardiaceae?). (A, B) MNHN.F.50234.1, transverse sections; (C–F) MNHN.F.50234.3, tangential longitudinal sections; (G–I), MNHN.F.50234.6, radial longitudinal sections. (A) Poorly preserved vessels, radially compressed. (B) Solitary vessels filled with orange-brown material. (C) Simple perforation plate and non-vestured intervessel pits. (D) Rays (1–2-seriate), axial parenchyma associated with vessels (arrowhead). (E) Detail of parenchyma strands with arrowheads pointing to end walls. (F) Rays (1–2-seriate) with obvious upright marginal cells (arrowheads). (G) Possible simple vessel-ray parenchyma pits. (H) Heterocellular rays with mostly square and upright cells (arrowhead). (I) Heterocellular ray with procumbent body cells (white arrowhead) and one marginal row of upright cells (black arrowhead). Scale bars: (A) 500 µm; (D, F, H) 200 µm; (B, I) 100 µm; (E) 50 µm; (C, G) 25 µm.
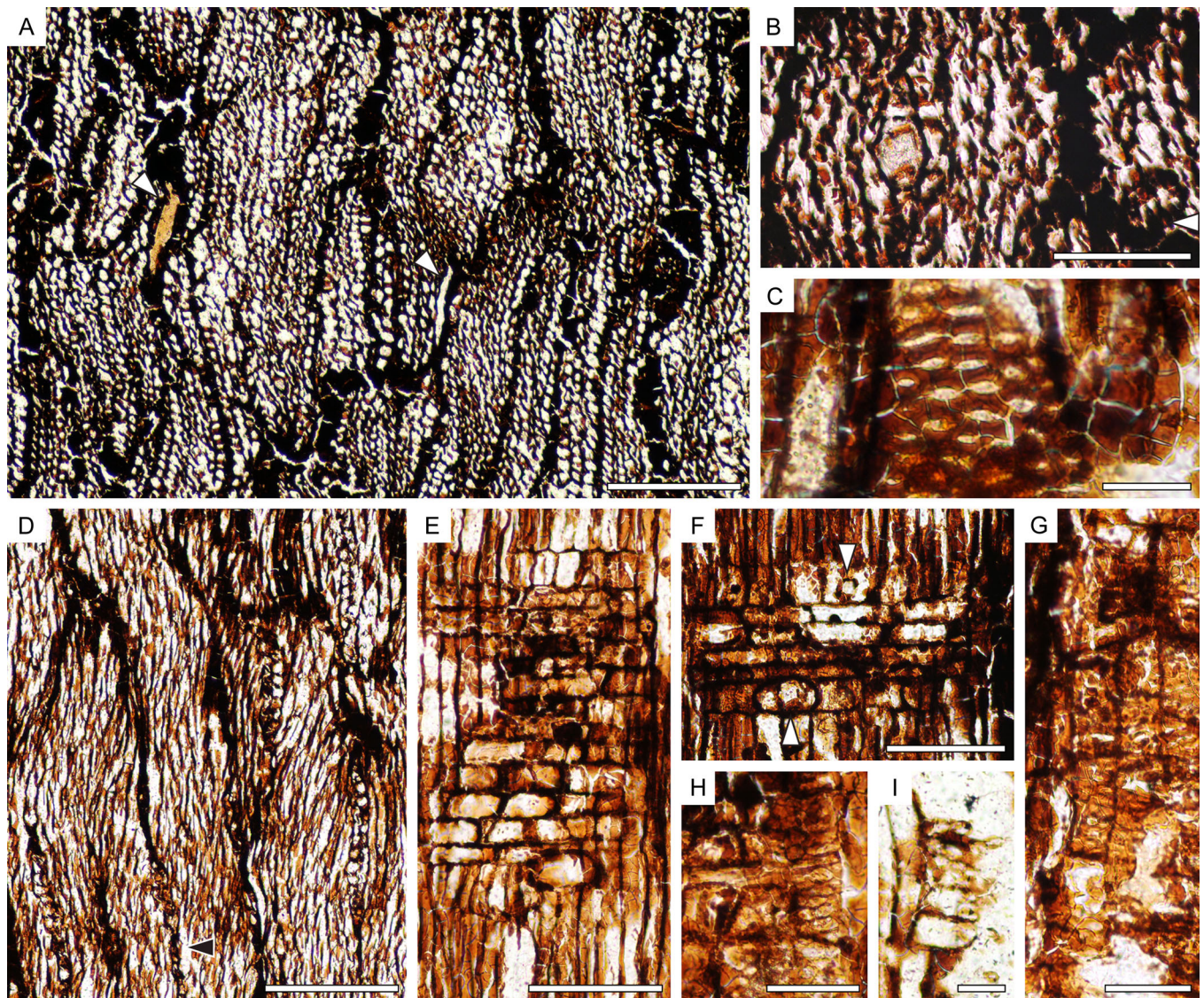
FIGURE 11 Wood-type 2-d (incertae sedis). (A, B) MNHN.F.50235.1, transverse sections; (C, E–G) MNHN.F.50235.5, radial longitudinal sections; (D) MNHN.F.50235.3, tangential longitudinal section. (A) Tangentially compressed wood, making it difficult to distinguish vessels (arrowheads). (B) Crystal in a ray parenchyma cell. (C) Large non-vestured intervessel pits. (D) Rays mostly 2-seriate but also uniseriate (arrowhead). (E) Heterocellular rays with procumbent cells and mostly 1 marginal row of upright cells. (F) Crystals in marginal ray cells (arrowheads); the bottom one is in an enlarged cell. (G) Vessel-axial parenchyma seemingly bordered pits. (H) Possible vessel-ray parenchyma pits, enlarged with reduced borders. (I) Possible vessel-ray parenchyma pits, with narrow borders. Scale bars: (A, D) 200 μm; (B, E, F) 100 μm; (C, I) 25 μm; (G, H) 50 μm.

(mean 22/mm²); tangential diameter 50–140 μm (mean 93 μm), radial diameter 40–140 μm (mean 88 μm). Tyloses sometimes present (Figure 12E). Vessel element length 340–715 μm (mean 500 μm) long. Perforation exclusively scalariform, 8–16 bars, occasionally forked (Figure 12L), bars 1.5–5.5 μm thick (mean 3.1 μm) and separated by 8–30 μm (mean 18 μm), the wider vessels have fewer bars and greater spaces between them. Intervessel pits alternate, with a faint tendency to a polygonal outline, non-vestured, 5–9 μm (mean 7 μm) wide, with round aperture (Figure 12G). Vessel-ray parenchyma pits and vessel-axial parenchyma pits likely similar in size and shape to intervessel pits (Figure 12H, K), with borders, sometimes reduced, 5–12 μm (mean 7 μm). Some larger pits are seen,

but their nature is ambiguous (Figure 12J). Parenchyma barely visible in transverse section, some unicellular tangential lines with some cells with different content than other cells could be parenchyma (Figure 12B). Axial parenchyma strands visible in radial section, likely diffuse to diffuse-in-aggregates (Figure 12C); parenchyma cells 70–200 μm (mean 139 μm) long, 16–30 μm (mean 22 μm) wide in tangential section; up to 6 cells per strand, maybe more; no crystals. Rays 1–6-(7-)seriate, mostly 1- and 3–4-seriate, (1-seriate: 23-29%, 2-seriate: 15%, 3-seriate: 25%, 4-seriate: 25%, 5-seriate: 4–9%, 6-seriate: 1–3%), 5–9 rays/mm (mean 7/mm), ray height 640–4100(5100) μm (mean 1840 μm) or 13–70(140) cells (Figure 12D, E); uniseriate rays can be as long as
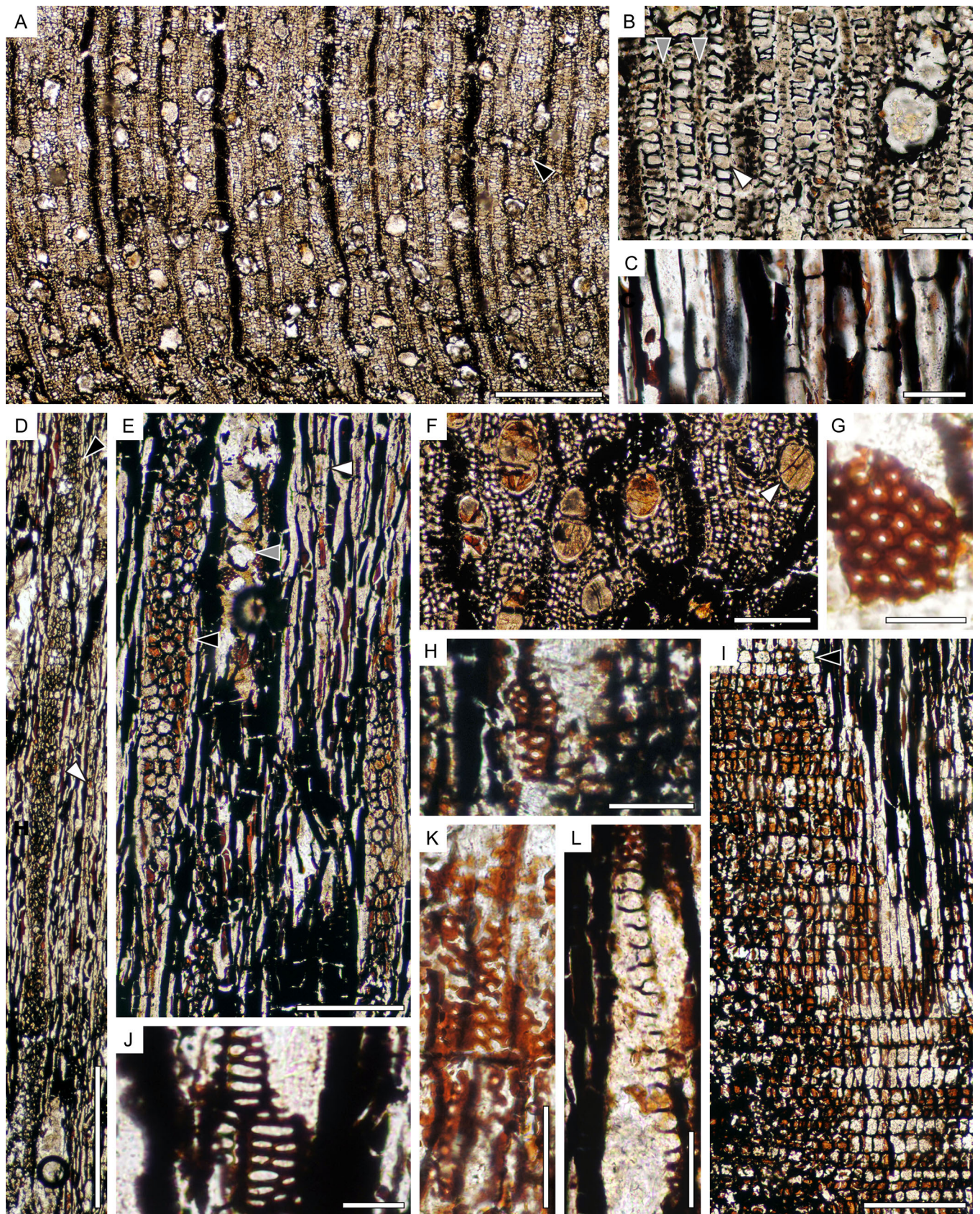
FIGURE 12 (See caption on next page).

multiseriate rays; homocellular to weakly heterocellular almost exclusively made of square or upright cells (Figure 12I); square cells are more common in the middle portion and upright cells at the ends forming uniseriate marginal rows that extend up to 8–13 cells; some rare procumbent cells occur in the middle of the rays (Figure 12I). Kribs's ray type heterogeneous I. Sheath cells are sometimes present (Figure 12E). Fibers apparently non-septate, radially aligned, 11–26 μm in tangential diameter (mean 18 μm), thin-to-thick walled (lumen about 1.2 times the double wall thickness) (Figure 12B).

Estimated minimal diameter—mean 7 cm (4–10 cm)

InsideWood code (fossil code in brackets)—2 5 14 15 16 22 25 26 30v 31v 41 42v 47 48 53 56v 66 69 77 78? 79? 93 94? 97 98 102 105 108v 109v 110 115 168 (300v 302 313 315)

Affinities and remarks

Results of a search of InsideWood (2004 onward) for diffuse porous wood (5p), scalariform perforation plates with <20 bars (14p, 17a, 18a), alternate intervessel pits (22p), >20 vessels/mm² (46a, 48p), diffuse or diffuse-in-aggregates parenchyma (76p/77p), larger rays >4-seriate and >1 mm high (96a, 98p, 102p) returned some Cornaceae (*Alangium* Lam.), Lecythidaceae, Myricaceae, and Phyllanthaceae (*Aporosa* Blume, *Baccaurea* Lour., *Wielandia* Baill.). Without any vessel density restriction, it adds Garryaceae (*Garrya* Douglas ex Lindl.), Sabiaceae (*Meliosma* Blume, although parenchyma is rare or scanty) and Styracaceae (*Styrax* L.). The combination of some of these features also occurs in Violaceae, Pandaceae, Putranjivaceae (*Putranjiva* Wall.), Symplocaceae (*Symplocos* Jacq.), Siparunaceae (*Siparuna* Aubl.), Celastraceae, and Stemonuraceae. Exclusively scalariform perforation plates with few bars, alternate intervessel pits, parenchyma diffuse-in-aggregates, and tall rays with mostly square and upright cells do not occur in combination in any of the families cited above. As a consequence, the present fossil could either be placed at the base of the asterids, close to Malpighiales, close to Proteales at the base of Eudicots, or even in Laurales.

In the fossil wood database of InsideWood, there are only a few descriptions for woods with alternate intervessel pits and scalariform perforation plates with relatively few bars. *Alangioxylon* Awasthi has diffuse to diffuse-in-aggregates parenchyma, sheath cells and rays up to 2250 μm high, but rays have procumbent cells in the median portion, perforation plates are both simple and scalariform and intervessel pits with linear apertures (Awasthi, 1969). *Alangium oregonensis* Scott & Wheeler has diffuse to diffuse-in-aggregates parenchyma, tall rays, similar ray size and density, but with mainly procumbent cells in the median portion, mostly only reaching 4-seriate, simple and scalariform perforation plates with fewer bars (1–10) (Scott and Wheeler, 1982). There are other fossil woods that partly share some features with our fossil: (1) the Upper Cretaceous Big Bend Ericalean Wood Type I (Wheeler and Lehman, 2009), (2) the Eocene Nut Beds Xylotype IB-3 (Wheeler and Manchester, 2002), (3) the Eocene Nut Beds Xylotype IA-1, (4) one specimen of Page's classification Group IIIB3 (Page, 1979). Only three fossils with scalariform perforation plates are described from the Deccan intertraps (Wheeler et al., 2017), but they do not resemble our fossil because of opposite pitting, narrow rays, and rare parenchyma (Bande and Khatri, 1980; Srivastava et al., 2019). Overall, the combination of few bars per scalariform perforation plates and alternate intervessel pits features rarely occurs. When it does, the parenchyma is less developed or the rays have mostly procumbent cells, which is not the case with our specimen. A new genus and species are thus created for this specimen: *Compitoxylon paleocenicum* gen. et sp. nov.

DISCUSSION

Deposition, preservation, and type of material

The fossil specimens have undergone various degrees of chemical and/or biological degradation, as well as some compression. The fragments are small with some rounded edges. They were found randomly dispersed without orientation in the tuffaceous material. Figure 1D shows that most of the plant debris of these tuffaceous beds are wood fragments; no leaves, large axes nor fruits were found. These taphonomic features suggest that a pyroclastic flow broke down and carbonized plant parts as it flowed downslope; it also recalls some of the volcanic deposits illustrated by Tosal et al. (2022: p. 9, fig. 6b). The estimated original diameters are between 4 and 15 cm on average. Larger plant parts, such as trunks, might have remained near their original location, while smaller branches (from young individuals, bushes or understorey trees) were more easily transported. Our set of specimens may thus represent a diverse range of ecosystems, from the volcano foothills to

FIGURE 12 *Compitoxylon paleocenicum* gen. et sp. nov. (incertae sedis). (A, B, F) MNHN.F.50236.1, transverse sections; (D, E) MNHN.F.50236.3, tangential longitudinal sections; (C, G–L) MNHN.F.50235.5, radial longitudinal sections. (A) Numerous small, mostly solitary vessels, sometimes anomalous holes (arrowhead). (B) Detail of radial vessel multiple of two, multiseriate rays, uniseriate rays (grey arrowheads), fibers and possible diffuse-in-aggregates axial parenchyma (white arrowhead). (C) Axial parenchyma strands, either diffuse-in-aggregates or diffuse; (D) Uniseriate ray (white arrowhead) and very high 5-seriate ray (black arrowhead). (E) Uniseriate ray (white arrowhead), multiseriate rays with long rows of marginal cells, sheath cells in 4-seriate ray (black arrowhead), tyloses in vessel (grey arrowhead). (F) Vessel solitary and in short radial multiples; one vessel shows a scalariform perforation plate (arrowhead). (G) Round to slightly polygonal non-vestured intervessel pits with round apertures. (H) Possible bordered vessel-ray pits. (I) High rays with mostly square and upright cells, also some almost square procumbent cells (arrowhead). (J) Vessel-ray parenchyma or vessel-axial parenchyma pits. (K) Bordered vessel-ray parenchyma pits (in upright cells). (L) Scalariform perforation plate with 16 bars, bars sometimes forked. Scale bars: (A, D) 500 μm; (E–F, I) 200 μm; (B, H) 100 μm; (C, J–L) 50 μm; (G) 25 μm.

the coast, with certain taxa potentially over-represented or eliminated.

Diversity of the assemblage

Monocotyledons

The identification of taxa within the Arecaceae family can be challenging, particularly when using the anatomy of the stipes (Thomas, 2011a). The variability within and among individuals can be significant and depend on factors such as the location within the stem. The presence of two distinct Arecaceae indicates a subtropical to tropical environment (Baker and Couvreur, 2013a). The family was already widespread in the Cretaceous with various centers of diversification and dispersal pathways in both Laurasia (e.g., Coryphoideae) and Gondwana (e.g., Arecoideae) (Baker and Couvreur, 2013a, b). Many palm fossils are known from the late Cretaceous–early Paleocene of India, including Coryphoideae (Srivastava et al., 2014). It has been suggested that the Indian Plate played a significant role in dispersal of the subfamily (Srivastava et al., 2014), though this hypothesis remains controversial (Baker and Couvreur, 2013b). Our fossils from the Burma Terrane, anchored to India at that time, corroborate the presence of palms in South Asian Paleocene ecosystems.

Dicotyledons

Some of our dicotyledenous specimens share similarities with Sapindales, especially with Anacardiaceae and Meliaceae. Anacardiaceae are pantropical from wet to dry ecosystems, with some species in temperate climates (Weeks et al., 2014). The precursor of Anacardiaceae (and particularly the *Mangifera-Gluta-Anacardium* group) has been proposed to have originated in tropical wet southeast Asia and to have expanded to Sub-Saharan Africa near the Cretaceous–Paleogene boundary (Weeks et al., 2014). Fossil woods from the Late Cretaceous to Eocene of North America and Europe and from the late Cretaceous-early Paleocene Deccan intertraps highlight the wide early distribution of the family (Gregory et al., 2009 and references therein; Weeks et al., 2014). Meliaceae are almost pantropical, with some representatives outside the tropics (Heads, 2019). They display very diverse morphologies and anatomies and are present in various climates, which implies that the family likely had a large ancestral geographic and climatic distribution (Heads, 2019). Moraceae are widely distributed and considered cosmopolitan from tropical rainforests to temperate areas (Zerega et al., 2005). Most species are found in tropical Asia and the Indo-Pacific Islands; they are thought to originate in Laurasia (Zerega et al., 2005). Fossil woods related to Moraceae are present in the Deccan intertraps (Mehrotra et al., 1984; Wheeler et al., 2017).

Combretaceae are pantropical, with *Terminalia* primarily found in Southeast Asia (Gere, 2013). The center of diversification of this genus is considered to be in Southeast Asia, although its origin, like the rest of the family, is believed to be in Africa (Gere, 2013).

Fabaceae occur worldwide and in almost every environment. The evolutionary history of Fabaceae is poorly understood, mostly due to their huge diversity in morphology, anatomy, and ecology and their wide distribution and difficulties in identifying their fragments in isolation. Widespread during the Eocene (Epihov et al., 2017), the scarcer Paleocene fossil record of Fabaceae indicates an earlier presence of the family in South America (Herrera et al., 2019) and Africa (Koeniguer et al., 1971; Crawley, 1988). The Indian Fabaceae of the late Paleocene–early Eocene suggest a dispersal from Africa to Asia during that time (Chandra et al., 2022; Bhatia et al., 2023).

Lauraceae are an old pantropical lineage, with few species outside the tropics. Their origin is both presumed in Gondwana and Laurasia (Chanderbali et al., 2001). Although the Gondwanan origin is favored, most of the modern Lauraceae are thought to come from Laurasian clades (Chanderbali et al., 2001). The fossil record of the family is large, mostly dated from the Eocene or later (Dupéron-Laudoueneix and Dupéron, 2005; Gregory et al., 2009; and references therein). A few Paleocene Lauraceae fossils are recorded in England (Crawley, 1989), the United States (Herendeen et al., 1994; Wheeler et al., 2019), Cameroon (Dupéron-Laudoueneix and Dupéron, 2005), and in ancient islands of the Indian Ocean (Carpenter et al., 2010) and Australia (Vadala and Greenwood, 2001), attesting that the family was already widespread at this time.

Implications

Sapindales and Arecaceae are frequent in the Deccan intertraps (in addition to Malpighiales and Malvales), which indicates some resemblance between our Burmese and the Deccan fossil wood assemblages. The possible affinity of the Wood-type 1-a and the Fabaceae is also consistent with the fact that Fabaceae are absent in the Deccan assemblages but present in younger Paleocene formations (although not as wood). Lauraceae are not reported in the Deccan assemblages. Awasthi and Jafar (1990) recorded poorly dated (likely Paleocene–Eocene) fossil wood attributed to Lauraceae from the Andaman-Nicobar Islands. They questioned the possible origin of the material from the nearby Burmese region, which would make, beside the Indian record, the closest record of possibly Paleocene wood from the Paunggyi Formation. Today's tropical to subtropical Myanmar ecosystems also include some Moraceae (*Artocarpus* J.R.Forst. & G.Forst.), Anacardiaceae (*Swintonia*), Ebenaceae (*Diospyros* L.), Rhamnaceae (*Ziziphus*), Combretaceae (*Terminalia*), Fabaceae (*Xylia* Benth.),

TABLE 1 Summary of the anatomical features of the nine specimens of dicotyledonous wood.

Group	Fossil	Growth ring boundary	Perf. plates	Vessel diam. (μm); density (/mm²); vessel outline	Solitary vessels (%); max. group	Vessel element (μm)	Intervessel pit diam. (μm)	Vessel-ray pits
1	1-a PPP0 Meliaceae/Fabaceae	Maybe	Simple	75–220 [130] 1–4 [2] oval to round	70 2[3]	188–307 [252]	Alternate; 3–6 [4]	Similar to IVP
	1-b PPP9 Moraceae/Sapindales	Maybe	Simple	44–184 [96] 4–23 [12] round to oval tyloses	68 2–3[6]	150–350 [225]	Alternate, non-vestured; 5.6–12 [8.6]	Reduced borders to simple, 5.3–14.5
	1-c PPP2 Sapindales?	Absent	Simple	35–190 [104] 3–8 [4] round to oval	80 2	125–280 [189]	Alternate, non-vestured; 3–6 [4.5]	?
	1-d PPP6 Lauraceae?	Absent?	Simple	45–170 [87] 5–11 [8] round	90 2–3	85–335 [195]	Alternate, non-vestured, ± enlarged; 7–11.5 [9.2]	Reduced borders to simple?
2	2-a PPP5 Anacardiaceae	Absent	Simple	50–225 [155] 3–9 [6] round tyloses	70–82 2–3[4]	190–445 [260]	Alternate, non-vestured; 5.8–13.5 [9]	Reduced borders to simple, 5–13
	2-b PPP7 Sapindales/Combretaceae?	Absent	Simple	r. 70–220 [140] 4–6? oval	95? 2	?	Alternate, non-vestured; 5.7–12.5 [9.6]	Reduced borders to simple 5–10.3
	2-c PPP8 Anacardiaceae?	Absent?	Simple	50–155 [105] 5–13 [6] round to oval	85 2	185–535 [305]	Alternate, non-vestured, ± enlarged; 6–12 [8.6]	Reduced borders?
	2-d PPP10 Inc. sed.	Absent	Simple	r. 60–170 [110] 4–10? oval	Mostly? -	142–320 [225]	Alternate, non-vestured, ± enlarged; 6–11.5 [8.1]	Similar to IVP? or reduced borders? 6–13
3	Compitoxylon paleocenicom gen. et sp. nov. Inc. sed.	Maybe	Scalarif., 8–16 bars	50–140 [93] 13–35 [22] round to oval (tyloses)	45–80 2–3[7]	340–715 [500]	Alternate, non-vestured, 5–9 [7], faintly polygonal	Similar to IVP (to reduced border), 5–12 μm

Fibers; pits diam. (μm)	Axial parenchyma	Ray composition	Ray width (cells)	Ray height (μm; cells)	Crystals (μm)	Estimated diameter (cm)	Other
Non-septate, radial rows, pits 2.5–5.6	Confluent-banded, aliform, 1–6-seriate bands, 2–7/mm, 2–4(6) cells/strand	Heterocellular, procumbent with 1 row of sq./up. cells, 5–9/mm	1–4(5)	95–580 [280] 4–29 [13] end-to-end con.	Parenchyma, 15–45 Rays?	5–6	–
Non-septate, radial rows, thin-to-thick walled (1:1)	Vasicentric, (diffuse?/ aliform?), 5(9) cells/strand	Heterocellular to weakly heterocellular, procumbent with 1(–2) rows of sq./up. cells (or enlarged procumbent), 2–6/mm	(1)2–4(5)	82–614 [265] 5–40 [17]	?	7.2–16.3	Branch trace, ray intercellular spaces

TABLE 1   (Continued)

Fibers; pits diam. (µm)	Axial parenchyma	Ray composition	Ray width (cells)	Ray height (µm; cells)	Crystals (µm)	Estimated diameter (cm)	Other
Non-septate, radial rows	Rare/scanty?	Heterocellular, procumbent with 1–3 rows of sq./up. cells, (also mixed throughout?), uniseriate with only sq./up.?, 5–12/mm	1–4	200–800 [370] 6–41 [19] up to 76?	–	12–16.5?	Sometimes ray intercellular spaces
Radial rows	Scanty/vasicentric; (diffuse?); 4 cells/ strands (or more)	Heterocellular, procumbent with 1–2 row of sq./up. cells (or mixed throughout?), 4–11/mm	(1)2–4(5)	100–1530 [470] 4–60 [21] end-to-end con.	?	5.6–8.3	Lacunae (oil cells?)
Non-septate?, radial rows	Scanty/vasicentric; 4 cells/ strands	Heterocellular, procumbent with 1–4 rows of sq./up. cells (or mixed throughout), 4–9/mm	1–2(3)	130–600 [260] 4–26 [10]	–	3–7?	Branch traces with helical thickening
Non-septate?, radial rows	Scanty/vasicentric	Heterocellular, procumbent with 1(–3) row of sq./up. cells, 5–12/mm	1(2)	87–720 [246] 2–30 [10]	Rays	4–7?	–
Non-septate, radial and tangential rows	Scanty/vasicentric	Heterocellular, procumbent (sometimes almost sq.) with 1–3 row of sq./up. cells, 2–7/mm	1–2(3)	123–475 [240] 3–17 [9]	–	5–7	–
Non-septate, radial rows	Scanty/vasicentric	Heterocellular, procumbent with 1(–3) rows of sq./up. cells, (uniseriate with only sq./up.), 3–7/mm	1–2(3)	63–450 [215] 4–21 [11]	Rays 23–27	?	–
Non-septate, radial rows, thin-to-thick walled (1:1.2)	Diffuse-in-aggregate, (or diffuse?), ~6 cells/ strand	Homocellular to weakly heterocellular, sq. (few proc.) with up to 8–13 rows of up. cells, uniseriate with only up. cells as long as multiseriate, 5–9/mm	1–4(6) frequent uniseriate, sheath cells	640–4100 [1840] up to 5100? 13–70 up to 140?	–	4–10	–

Notes: () = occasional, [] = mean values, ? = uncertain, r. = radial diameter, Inc. sed. = Incertae sedis, perf. = perforation, scalarif. = scalariform, diam. = diameter, max. = maximum, sq. = square, up. = upright, proc. = procumbent, con. = connection.

several species of Meliaceae, Sabiaceae, a few Burseraceae, and species of palms (Kress et al., 2003). Therefore, our assemblage indicates a long-lasting regional presence of Sapindales, Arecaceae, and possibly Moraceae and Fabaceae. However, one of the present-day dominant families of Southeast Asian forests (Dipterocarpaceae) has not been identified here.

Anacardiaceae, Arecaceae-Coryphoideae, and Moraceae are believed to have originated in Laurasia (Zerega et al., 2005; Baker and Couvreur, 2013a; Weeks et al., 2014). Their presence in suggests floral exchanges between Eurasia and Myanmar (and adjacent India) as early as the mid Paleocene. By contrast, families that dispersed and diversified within India, in relation to the Africa–India floristic interchanges, such as the Dipterocarpaceae (Bansal et al., 2022) have not been identified. Fossils of dipterocarps are rare in the Paleogene records in comparison to the Neogene. They are present in the Deccan intertraps only as leaves (Khan et al., 2020). The earliest records of dipterocarps are pollen from the Maastrichian in Sudan (Bansal et al., 2022) and the late Paleocene/early Eocene in India (Prasad et al., 2009; Bansal et al., 2022). The earliest reference of dipterocarp wood is from the lower Eocene in India (Rust et al., 2010), though these fossils are poorly preserved, and from the middle Eocene in Myanmar (Licht et al., 2014). There are various explanations for this apparent scarcity including (1) the presence of dipterocarps in environments that are poorly represented in the fossil record (distal floodplains, foothills, or higher altitudes); (2) the minor presence of dipterocarps in the floral assemblage, so they are not represented at the Paleocene sites due to the limited amount of samples; (3) the volcanic events may not have impacted dipterocarp trees the same way as the flora sampled here, as they are typically taller than other trees; (4) the family's initial evolution may have involved a prolonged period of mosaic evolution, (5) early fossils might have lacked distinctive anatomical characteristics of the dipterocarps. Unless a fossil wood is well preserved it can be difficult to see important diagnostic features of the Dipterocarpaceae such as vasicentric tracheids and secretory canals (which may be absent, as seen for canals in the Monoteoideae subfamily).

Anatomical interpretations and functional traits

Ecological interpretations

A summary of the anatomical features of our dicotyledonous specimens is presented in Table 1. Several features of the assemblage support an origin from branches or axes of small individuals, such as understorey trees or bushes, growing under everwet tropical conditions.

Tending to narrow vessels (between 80 μm and 100 μm in average diameter in some of our specimens) and short vessel elements (<350 μm in average for eight of nine dicot specimens) is commonly associated with small individuals, branches, bushes, or plants growing in seasonal to dry area

(Lindorf, 1994; Baas et al., 1983, 2004; Carlquist, 2012). Shorter vessel elements are more common in juvenile wood (close to pith) than in mature wood (e.g., Baas, 1976). The small size of the closely spaced nodes found in Type 2-a also suggests that it came from a small branch. Palm species with mostly one large vessel or with large vessels (>183 μm of diameter, as for *Palmoxylon* sp.1 and *Palmoxylon* sp. 2) are mostly represented in tropical rainforests (Thomas and Boura, 2015). The presence of faint growth-ring boundaries in Wood-type 1-a, 1-b, and *Compitoxylon paleocenicum* gen. et sp. nov. suggest that the water availability is not uniform throughout the year. However, the medium to large non-vestured intervessel pits in six specimens indicate that water stress was limited. Indeed, large, non-vestured pits are considered less safe against embolism and water stress than small or vestured pits (Lindorf, 1994; Carlquist, 2001; Wheeler et al., 2007; Silva et al., 2021). Scalariform perforations are more common in mesic environments or those with low temperature and low evaporation (Baas, 1976). At present-day tropical latitudes, some species display scalariform perforation plates (about 10%), although less frequently than at temperate latitudes (about 20%; Wheeler and Baas, 2019). Scalariform perforation plates can be present within lineages that mostly display simple perforation plates and are common in specific lineages (cf. Myristicaceae, basal clades such as Magnoliaceae or basal asterids such as Cornales and Ericales). The presence of scalariform perforation plates (with few bars) in *Compitoxylon paleocenicum* gen. et sp. nov. is consistent with the hypothesis of an environment with a steady water supply. Finally, parenchyma is generally more commonly paratracheal in tropical floras than in flora of higher latitudes where it is mainly apotracheal (e.g., Wheeler et al., 2007; Morris et al., 2016).

Evolutionary trends

Our assemblage displays many "modern" features such as marginal and aliform-confluent axial parenchyma, alternate intervessel pits, exclusively uniseriate rays, rays weakly heterocellular, and dominantly simple perforation plates (see Wheeler and Baas, 2019). "Primitive" features such as scalariform perforation plates (11% compared to 3% in the Deccan, 10–45% in other Paleocene localities), tall rays (>1 mm) with almost exclusively square and upright cells, numerous narrow vessels, long vessel elements and diffuse-in-aggregates parenchyma are also found. Thus, "primitive" and "modern" features are present in both the assemblage and within the same specimens (as in *C. paleocenicum* gen. et sp. nov.). The anatomical diversity of our assemblage is high but not very different from modern ones or the assemblage of intertrappean beds (Wheeler et al., 2017; Wheeler and Baas, 2019). Our findings thus support the observations of Wheeler et al. (2017) and Wheeler and Baas (2019) suggesting that low-latitude tropical flora display modern-

like anatomical diversity earlier than other floras. The high anatomical diversity of our relatively small assemblage supports the hypothesis that low latitudes favor the diversification of wood anatomy, but it remains unclear if they work as a "cradle" of diversification (a source of new features), or as a "museum" (existing features are maintained even in few proportions).

CONCLUSIONS

Our Paleocene assemblage includes relatives of Arecaceae, Sapindales, Rosales and possibly Fabales, Myrtales, Malpighiales, Proteales, and even Laurales. Most specimens are likely branches or small axes, transported by a volcanic event. They indicate a tropical environment with limited seasonal water stress, as expected at low latitudes. Anacardiaceae, Arecaceae-Coryphoideae, and Moraceae identified here are of supposed Laurasian origin; these affinities indicate the early dispersal of Laurasian elements into the Burma Terrane and adjacent India. Families that are widespread in modern South Asian forests (i.e., Dipterocarpacae and Fabaceae) or are thought to have dispersed as early as the Paleocene to India (Dipterocarpaceae) have not been identified, suggesting that "modern" South Asian rainforests emerged later in the Cenozoic. The anatomical diversity of our assemblage corroborates that tropical flora display "modern" features early in the history of angiosperms and that their high diversity remained steady through time; low latitudes might have thus accelerated adaptive xylem evolution. It is thus crucial to further investigate low-latitude Paleocene assemblages because they represent key elements to understand the biogeography of tropical lineages as well as the early evolution and diversification of wood anatomy.

AUTHOR CONTRIBUTIONS

A.L., Z.W., D.W.A., and G.D.N. collected the specimens; A.L. dated the volcanic bed yielding the fossil specimens; N.G. described and identified the specimens with inputs from D.D.F. and A.B.; N.G. developed figures and tables; A.L. and N.G. wrote the introduction; A.L. wrote the geological context section; all other sections were written by N.G. with input from A.L., D.D.F., and A.B.; all authors revised the manuscript.

ACKNOWLEDGMENTS

DATA AVAILABILITY STATEMENT

All microscopic slides are deposited and available at the MNHN and the remains of the original specimens until further restitution to the collection of the Department of Geology at the University of Yangon (Myanmar). All voucher numbers with links to the MNHN collection database are listed in the Appendix 1. The raw and full-resolution versions of the individual photos used in the figures and additional photos are available in the InDoRES Data Repository: https://doi.org/10.48579/PRO/YTWOSL (Gentis, 2023).

ORCID

Nicolas Gentis https://orcid.org/0000-0003-1414-1237
Alexis Licht https://orcid.org/0000-0002-5267-7545
Dario De Franceschi https://orcid.org/0000-0002-0570-060X
Day Wa Aung https://orcid.org/0000-0002-4346-3633
Guillaume Dupont-Nivet https://orcid.org/0000-0001-9905-9739
Anaïs Boura https://orcid.org/0000-0002-3144-8217

REFERENCES

Agarwal, A. 1988. Occurrence of *Bouea* in the Neyveli Lignite deposits, India. *Geophytology* 18: 166–168.

Akhmetiev, M. A. 2007. Paleocene and Eocene floras of Russia and adjacent regions: climatic conditions of their development. *Paleontological Journal* 41: 1032–1039.

Angiosperm Phylogeny Group [APG IV]. 2016. An update of the Angiosperm Phylogeny Group classification for the orders and families of flowering plants: APG IV. *Botanical Journal of the Linnean Society* 181: 1–20.

Awasthi, N. 1966. Fossil woods of Anacardiaceae from the Tertiary of South India. *Palaeobotanist* 14: 131–143.

Awasthi, N. 1969. A new fossil wood belonging to the family Alangiaceae from the Tertiary of South India. *Palaeobotanist* 17: 322–325.

Awasthi, N. 1974. Neogene angiospermous woods. *In* K. R. Surange, R. N. Lakhanpal, and D. C. Bharadwaj [eds.], Aspects and appraisal of Indian palaeobotany, 341–358. Birbal Sahni Institute of Palaeobotany, Lucknow, India.

Awasthi, N. 1989. Occurrence of *Bischofia* and *Antiaris* in Namasang beds (Miocene-Pliocene) near Deomali, Arunachal Pradesh, with remarks on the identification of fossil woods referred to *Bischofia*. *Palaeobotanist* 37: 147–151.

Awasthi, N., and A. Jafar. 1990. First fossil wood (Lauraceae) from Baratang, Andaman-Nicobar Islands, India. *Current Science* 59: 1243–1244.

Awasthi, N., and R. C. Mehrotra. 1990. Some fossil woods from Tipam Sandstone of Assam and Nagaland. *Palaeobotanist* 38: 277–284.

Awasthi, N., and U. Prakash. 1987. Fossil woods of *Kingiodendron* and *Bauhinia* from the Namsang beds of Deomali, Arunachal Pradesh. *Palaeobotanist* 35: 178–183.

Baas, P. 1976. Some functional and adaptative aspects of vessel member morphology. *Leiden Botanical Series* 3:157–181.

Baas, P., F. W. Ewers, S. D. Davis, and E. A. Wheeler. 2004. Evolution of xylem physiology. *In* A. R. Hemsley and I. Poole [eds.], The evolution of plant physiology, 273–295. Elsevier Academic Press, London, UK.

Baas, P., E. Werker, and A. Fahn. 1983. Some ecological trends in vessel characters. *IAWA Journal* 4: 141–159.

Bailey, I. W., and W. W. Tupper. 1918. Size variation in tracheary cells: I. A comparison between the secondary xylems of vascular cryptogams, gymnosperms and angiosperms. *Proceedings of the American Academy of Arts and Sciences* 54: 149.

Baker, W. J., and T. L. P. Couvreur. 2013a. Global biogeography and diversification of palms sheds light on the evolution of tropical lineages. I. Historical biogeography. *Journal of Biogeography* 40: 274–285.

Baker, W. J., and T. L. P. Couvreur. 2013b. Global biogeography and diversification of palms sheds light on the evolution of tropical lineages. II. Diversification history and origin of regional assemblages. *Journal of Biogeography* 40: 286–298.

Bande, M. B., and S. K. Khatri. 1980. Some more fossil woods from the Deccan Intertrappean beds of Mandla District, Madhya Pradesh, India. *Palaeontographica Abteilung B* 173: 147–165.

Bande, M. B., and U. Prakash. 1984. Evolutionary trends in the secondary xylem of woody dicotyledons from the Tertiary of India. *Palaeobotanist* 32: 44–75.

Bansal, M., R. J. Morley, S. K. Nagaraju, S. Dutta, A. K. Mishra, J. Selveraj, S. Kumar, et al. 2022. Southeast Asian dipterocarp origin and diversification driven by Africa–India floristic interchange. *Science* 375: 455–460.

Bender, F. 1983. Geology of Burma. Gebrüder Borntraeger, Berlin, Germany.

Bernaola, G., J. I. Baceta, X. Orue-Etxebarria, L. Alegret, J. Arostegui, and J. Dinarès-Turell. 2008. The mid-Paleocene biotic event at the Zumaia section (western Pyrenees): evidence of an abrupt environmental disruption. *Geophysical Research Abstracts* 10.

Bhatia, H., G. Srivastava, and R. C. Mehrotra. 2023. Legumes from the Paleocene sediments of India and their ecological significance. *Plant Diversity* 45: 199–210.

Bolotov, I. N., R. Pasupuleti, N. V. S. Rao, S. K. Unnikrishnan, N. Chan, Z. Lunn, A. V. Kondakov, et al. 2022. Oriental freshwater mussels arose in East Gondwana and arrived to Asia on the Indian Plate and Burma Terrane. *Scientific Reports* 12: 1518.

Bonde, S. D. 2008. Indian fossil monocotyledons: current status, recent developments and future directions. *Palaeobotanist* 57: 141–164.

Cai, F., L. Ding, Q. Zhang, D. A. Orme, H. Wei, J. Li, J. Zhang, et al. 2019. Initiation and evolution of forearc basins in the Central Myanmar Depression. *GSA Bulletin* 132: 1066–1082.

Carlquist, S. 2001. Comparative wood anatomy. Springer, Berlin, Germany.

Carlquist, S. 2012. How wood evolves: a new synthesis. *Botany* 90: 901–940.

Carpenter, R. J., E. M. Truswell, and W. K. Harris. 2010. Lauraceae fossils from a volcanic Palaeocene oceanic island, Ninetyeast Ridge, Indian Ocean: Ancient long-distance dispersal? *Journal of Biogeography* 37: 1202–1213.

Carvalho, M. R., C. Jaramillo, F. de la Parra, D. Caballero-Rodríguez, F. Herrera, S. Wing, B. L. Turner, et al. 2021. Extinction at the end-Cretaceous and the origin of modern Neotropical rainforests. *Science* 372: 63–68.

Chanderbali, A. S., H. Van Der Werff, and S. S. Renner. 2001. Phylogeny and historical biogeography of Lauraceae: Evidence from the chloroplast and nuclear genomes. *Annals of the Missouri Botanical Garden* 88: 104.

Chandra, K., A. Shukla, and R. C. Mehrotra. 2022. Early Paleogene megaflora of the palaeoequatorial climate: a case study from the Gurha lignite mine of Rajasthan, western India. *In* B. Phartiyal, R. Mohan, S. Chakraborty, V. Dutta, and A. K. Gupta [eds.], Climate change and environmental impacts: past, present and future perspective, Society of Earth Scientists series, 21–31. Springer International, Cham, Switzerland.

Chowdhury, K. 1936. A fossil dicotyledonous wood from Assam. *Annals of Botany* 50: 501–510.

Crawley, M. 1988. Palaeocene wood from the Republic of Mali. *Bulletin of the British Museum (Natural History) Geology* 44: 3–14.

Crawley, M. 1989. Dicotyledonous wood from the Lower Tertiary of Britain. *Palaeontology* 32: 597–622.

Crawley, M. 2001. Angiosperm woods from British Lower Cretaceous and Palaeogene deposits. *Special Papers in Palaeontology* 66: 1–100.

De Franceschi, D., C. Hoorn, P.-O. Antoine, I. U. Cheema, L. J. Flynn, E. H. Lindsay, L. Marivaux, et al. 2008. Floral data from the mid-Cenozoic of central Pakistan. *Review of Palaeobotany and Palynology* 150: 115–129.

Ding, L., P. Kapp, and X. Wan. 2005. Paleocene–Eocene record of ophiolite obduction and initial India-Asia collision, south central Tibet. *Tectonics* 24: TC3001.

Du, N. 1988. Fossil wood from the Late Tertiary of Burma. *Proceedings of the Koninklijke Nederlandse Akademie van Wetenschappen, B* 91: 213–236.

Dufraisse, A., J. Bardin, L. Picornell-Gelabert, S. Coubray, M. S. García-Martínez, M. Lemoine, and S. Vila Moreiras. 2020. Pith location tool and wood diameter estimation: Validity and limits tested on seven taxa to approach the length of the missing radius on archaeological wood and charcoal fragments. *Journal of Archaeological Science: Reports* 29: 102166.

Dupéron, J. 1975. Contribution à l'étude des flores fossiles de l'Agenais. Ph.D. dissertation, Université Pierre et Marie Curie, Paris, France.

Dupéron-Laudoueneix, M. 1980. Présence d'un bois fossile de Moraceae dans l'Eocène de la Charente. Section des Sciences, 117–129. Bibliothèque Nationale, Caen, France.

Dupéron-Laudoueneix, M., and J. Dupéron. 2005. Bois fossiles de Lauraceae: nouvelle découverte au Cameroun, inventaire et discussion. *Annales de Paléontologie* 91: 127–151.

Epihov, D. Z., S. A. Batterman, L. O. Hedin, J. R. Leake, L. M. Smith, and D. J. Beerling. 2017. N_2-fixing tropical legume evolution: a contributor to enhanced weathering through the Cenozoic? *Proceedings of the Royal Society, B, Biological Sciences* 284: 20170370.

Estrada-Ruiz, E., H. I. Martínez-Cabrera, and S. R. S. Cevallos-Ferriz. 2010. Upper Cretaceous woods from the Olmos Formation (late Campanian-early Maastrichtian), Coahuila, Mexico. *American Journal of Botany* 97: 1179–1194.

Franco, M. J. 2010. *Soroceaxylon entrerriensis* gen. et sp. nov. (Moraceae) de la Formación Ituzaingó (Plioceno-Pleistoceno), Cuenca del río Paraná, Argentina. *Revista Mexicana de Ciencias Geológicas* 27: 508–519.

Gasson, P., C. Trafford, and B. Matthews. 2003. Wood anatomy of Caesalpinioideae. *In* B. B. Klitgaard and A. Bruneau [eds.], Advances in legume systematics, vol. 10, 63–93. Royal Botanic Gardens, Kew, UK.

Gentis, N. 2023. Image library for: First fossil woods and palm stems from the mid Paleocene of Myanmar and their implications on biogeography and wood anatomy. *data.InDoRES* Website: https://doi.org/10.48579/PRO/YTWOSL

Gentis, N., A. Licht, A. Boura, D. De Franceschi, Z. Win, D. Wa Aung, and G. Dupont-Nivet. 2022. Fossil wood from the lower Miocene of Myanmar (Natma Formation): palaeoenvironmental and biogeographic implications. *Geodiversitas* 44: 853–909.

Gentry, A. H. 1992. Tropical forest biodiversity: distributional patterns and their conservational significance. *Oikos* 63: 19–28.

Gere, J. 2013. Combretaceae: phylogeny, biogeography and DNA barcoding. Ph.D. dissertation, University of Johannesburg, South Africa.

Gottwald, H. P. J. 1994. Tertiäre Kieselhölzer aus dem Chindwinn-Bassin im nordwestlichen Myanmar (Birma). *Documenta Naturae* 86: 1–90.

Gottwald, H. P. J. 1997. Alttertiäre Kieselhölzer aus miozänen Schottern der ostbayerischen Molasse bei Ortenburg. *Documenta Naturae* 109: 1–83.

Gradstein, F. M., J. G. Ogg, M. D. Schmitz, and G. M. Ogg [eds.]. 2020. Geologic time scale 2020. Elsevier, Amsterdam, Netherlands.

Gregory, M., I. Poole, and E. A. Wheeler. 2009. Fossil dicot wood names: an annotated list with full bibliography. *IAWA Journal* Supplement 6: 1–220.

Guleria, J. S. 1984. Leguminous woods from the Tertiary of District Kachchh, Gujrat, Western India. *Palaeobotanist* 31: 238–254.

Gupta, K. M. 1935. Critical remarks on *Dipterocarpoxylon burmense* Holden: *Irrawadioxylon* gen. nov. *Proceedings of the Indian Academy of Sciences, Section B* 1: 549–555.

Hass, H., and N. P. Rowe. 1999. Thin sections and wafering. *In* T. P. Jones and N. P. Rowe [eds.], Fossil plants and spores: modern techniques, 76–81. Geological Society, London, UK.

Heads, M. 2019. Biogeography and ecology in a pantropical family, the Meliaceae. *Gardens' Bulletin Singapore* 71: 335–461.

Herendeen, P. S., W. L. Crepet, and K. C. Nixon. 1994. Fossil flowers and pollen of Lauraceae from the Upper Cretaceous of New Jersey. *Plant Systematics and Evolution* 189: 29–40.

Herrera, F., M. R. Carvalho, S. L. Wing, C. Jaramillo, and P. S. Herendeen. 2019. Middle to Late Paleocene Leguminosae fruits and leaves from Colombia. *Australian Systematic Botany* 32: 385–408.

Hill, J. L., and R. A. Hill. 2001. Why are tropical rain forests so species rich? Classifying, reviewing and evaluating theories. *Progress in Physical Geography: Earth and Environment* 25: 326–354.

Huang, H., R. Morley, A. Licht, G. Dupont-Nivet, F. Grímsson, R. Zetter, J. Westerweel, et al. 2020. Eocene palms from central Myanmar in a South-East Asian and global perspective: evidence from the palynological record. *Botanical Journal of the Linnean Society* 194: 177–206.

Hyland, E. G., N. D. Sheldon, and J. M. Cotton. 2015. Terrestrial evidence for a two-stage mid-Paleocene biotic event. *Palaeogeography, Palaeoclimatology, Palaeoecology* 417: 371–378.

IAWA Committee. 1989. IAWA list of microscopic features for hardwood identification, E. A. Wheeler, P. Baas, and P. E. Gasson [eds.]. IAWA Bulletin new series 10: 219–332.

InsideWood. 2004 onward. Published on the Internet. Website: http://insidewood.lib.ncsu.edu/search.

Jaramillo, C., D. Ochoa, L. Contreras, M. Pagani, H. Carvajal-Ortiz, L. M. Pratt, S. Krishnan, et al. 2010. Effects of rapid global warming at the Paleocene–Eocene boundary on neotropical vegetation. *Science* 330: 957–961.

Jehle, S., A. Bornemann, A. Deprez, and R. P. Speijer. 2015. The impact of the Latest Danian event on planktic foraminiferal faunas at ODP Site 1210 (Shatsky Rise, Pacific Ocean). *PLoS ONE* 10: e0141644.

Kaiser, P. 1880. *Ficoxylon bohemicum*. Ein neues fossiles Laubholz. *Zeitschrift für die gesammten Naturwissenschaft* 53: 309–317.

Khan, M. A., R. A. Spicer, T. E. V. Spicer, K. Roy, M. Hazra, T. Hazra, S. Mahato, et al. 2020. *Dipterocarpus* (Dipterocarpaceae) leaves from the K-Pg of India: a Cretaceous Gondwana presence of the Dipterocarpaceae. *Plant Systematics and Evolution* 306: 90.

Koek-Noonnan, J., S. M. C. Topper, and B. J. H. ter Welle. 1984a. The systematic wood anatomy of the Moraceae (Urticales) I. Tribe Castilleae. *IAWA Journal* 5: 183–195.

Koek-Noonnan, J., S. M. C. Topper, and B. J. H. ter Welle. 1984b. The systematic wood anatomy of the Moraceae (Urticales) III. Tribe Ficeae. *IAWA Journal* 5: 330–334.

Koeniguer, J. C., D. E. Russel, and L. Thaler. 1971. Sur les bois fossiles du Paléocène de Sessao (Niger). *Review of Palaeobotany and Palynology* 12: 303–323.

Kramer, K. 1974. Die tertiären Hölzer Südost-Asiens (unter Ausschluß der Dipterocarpaceae) 1. Teil. *Palaeontographica Abteilung B* 144: 45–181.

Kress, W. J., R. A. DeFilipps, E. Farr, and D. Y. Y. Kyi. 2003. A checklist of the trees, shrubs, herbs, and climbers of Myanmar. *Contributions from the United States National Herbarium* 45: 1–590.

Legume Phylogeny Working Group (LPWG). 2017. A new subfamily classification of the Leguminosae based on a taxonomically comprehensive phylogeny. *Taxon* 66: 44–77.

Lemoigne, Y. 1978. Flores tertiaires de la haute vallée de l'Omo (Ethiopie). *Palaeontographica Abteilung B* 165: 89–157.

Lemoigne, Y., J. Beauchamp, and E. Samuel. 1974. Étude paléobotanique des dépots volcaniques d'âge tertiaire des bordures Est et Ouest du système des rifts éthiopiens. *Geobios* 7: 267–288.

Licht, A., A. Boura, D. De Franceschi, S. Ducrocq, A. Naing Soe, and J.-J. Jaeger. 2014. Fossil woods from the late middle Eocene Pondaung Formation, Myanmar. *Review of Palaeobotany and Palynology* 202: 29–46.

Licht, A., A. Boura, D. De Franceschi, T. Utescher, C. Sein, and J.-J. Jaeger. 2015. Late middle Eocene fossil wood of Myanmar: Implications for the landscape and the climate of the Eocene Bengal Bay. *Review of Palaeobotany and Palynology* 216: 44–54.

Licht, A., L. Reisberg, C. France-Lanord, A. Naing Soe, and J.-J. Jaeger. 2016. Cenozoic evolution of the central Myanmar drainage system:

insights from sediment provenance in the Minbu Sub-Basin. *Basin Research* 28: 237–251.

Lindorf, H. 1994. Eco-anatomical wood features of species from a very dry tropical forest. *IAWA Journal* 15: 361–376.

Mädel-Angeliewa, E., and W. R. Müller-Stoll. 1973. Kritische Studien über fossile Combretaceen-Hölzer: Über Hölzer vom Typus *Terminalioxylon* G. Schönfeld mit einer Revision der bisher zu *Evodioxylon* Chiarugi gestellten Arten. *Palaeontographica Abteilung B* 142: 117–136.

Martin, C. R., O. Jagoutz, R. Upadhyay, L. H. Royden, M. P. Eddy, E. Bailey, C. I. O. Nichols, and B. P. Weiss. 2020. Paleocene latitude of the Kohistan–Ladakh arc indicates multistage India–Eurasia collision. *Proceedings of the National Academy of Sciences, USA* 117: 29487–29494.

Martínez-Cabrera, H. I., and S. R. S. Cevallos-Ferriz. 2006. *Maclura* (Moraceae) wood from the Miocene of the Baja California Peninsula, Mexico: Fossil and biogeographic history of its closer allies. *Review of Palaeobotany and Palynology* 140: 113–122.

Martínez-Cabrera, H. I., S. R. S. Cevallos-Ferriz, and I. Poole. 2006. Fossil woods from early Miocene sediments of the El Cien Formation, Baja California Sur, Mexico. *Review of Palaeobotany and Palynology* 138: 141–163.

Mehrotra, R. C., U. Prakash, and M. B. Bande. 1984. Fossil woods of *Lophopetalum* and *Artocarpus* from the Deccan Intertrappean beds of Mandla District, Madhya Pradesh, India. *Palaeobotanist* 32: 310–320.

Menon, V. K. 1964. A new species of *Palmoxylon* from the Deccan Intertrappean Beds. *Proceedings of the Indian Academy of Sciences, B* 59: 77–87.

Metcalfe, C. R., and L. Chalk. 1950. Anatomy of the dicotyledons. Clarendon Press, Oxford, UK.

Mittelbach, G. G., D. W. Schemske, H. V. Cornell, A. P. Allen, J. M. Brown, M. B. Bush, S. P. Harrison, et al. 2007. Evolution and the latitudinal diversity gradient: speciation, extinction and biogeography. *Ecology Letters* 10: 315–331.

Morley, R. J. 2000. Origin and evolution of tropical rain forests. Wiley, Chichester, UK.

Morris, H., L. Plavcová, P. Cvecko, E. Fichtler, M. A. F. Gillingham, H. I. Martínez-Cabrera, D. J. McGlinn, et al. 2016. A global analysis of parenchyma tissue fractions in secondary xylem of seed plants. *New Phytologist* 209: 1553–1565.

Muellner-Riehl, A. N., A. Weeks, J. W. Clayton, S. Buerki, L. Nauheimer, Y.-C. Chiang, S. Cody, and S. K. Pell. 2016. Molecular phylogenetics and molecular clock dating of Sapindales based on plastid *rbcL*, *atpB* and *trnL-trnF* DNA sequences. *Taxon* 65: 1019–1036.

Ogata, K., T. Fujii, H. Abe, and P. Baas. 2008. Identification of the timbers of Southeast Asia and the Western Pacific. Kaiseisha Press, Ōtsu-shi, Japan.

Pace, M. R., C. S. Gerolamo, J. G. Onyenedum, T. Terrazas, M. P. Victorio, I. L. Cunha Neto, and V. Angyalossy. 2022. The wood anatomy of Sapindales: diversity and evolution of wood characters. *Brazilian Journal of Botany* 45: 283–340.

Page, V. M. 1979. Dicotyledonous wood from the Upper Cretaceous of Central California. *Journal of the Arnold Arboretum* 60: 323–349.

Pennington, R. T., M. Hughes, and P. W. Moonlight. 2015. The origins of tropical rainforest hyperdiversity. *Trends in Plant Science* 20: 693–695.

Pennington, T. D., and B. T. Styles. 1975. A generic monograph of the Meliaceae. *Blumea: Biodiversity, Evolution and Biogeography of Plants* 22: 419–540.

Pérez-Lara, D. K., E. Estrada-Ruiz, and C. Castañeda-Posadas. 2019. New fossil woods of Fabaceae from El Bosque Formation (Eocene), Chiapas, Mexico. *Journal of South American Earth Sciences* 94: 102202.

Poole, I. 2000. Fossil angiosperm wood: its role in the reconstruction of biodiversity and palaeoenvironment. *Botanical Journal of the Linnean Society* 134: 361–381.

Prakash, U. 1965a. *Dipterocarpoxylon tertiarum* sp. nov., a new fossil wood from the Tertiary of Burma. *Current Science* 34: 254–255.

Prakash, U. 1965b. Fossil wood of Dipterocarpaceae from the Tertiary of Burma. *Current Science* 34: 181–182.

Prakash, U. 1965c. Fossil wood of *Lagerstroemia* from the Tertiary of Burma. *Current Science* 34: 484–485.

Prakash, U. 1973. Fossil woods from the Tertiary of Burma. *Palaeobotanist* 20: 48–70.

Prakash, U. 1976. Fossil woods resembling *Dichrostachys* and *Entandrophragma* from the Tertiary of the Middle East. *Abhandlungen des Zentralen Geologischen Instituts* 26:499–507.

Prakash, U. 1979. Fossil wood of Dracontomelum from Lower Siwalik beds of Himachal Pradesh, India. *Geophytology* 8: 248–249.

Prakash, U., and N. Awasthi. 1970. Fossil woods from the Tertiary of Eastern India. 1. *Palaeobotanist* 18: 32–44.

Prakash, U., and M. B. Bande. 1980. Some more fossil woods from the Tertiary of Burma. *Palaeobotanist* 26: 261–278.

Prakash, U., and R. Dayal. 1965. Fossil wood resembling *Semecarpus* from the Deccan Intertrappean beds of Mahurzari near Nagpur. *Palaeobotanist* 13: 158–162.

Prakash, U., and P. P. Tripathi. 1976. Fossil dicot woods from the Tertiary of Assam. *Palaeobotanist* 23: 82–88.

Prasad, M., A. Agarwal, and B. D. Mandaokar. 2009. New species of the genus *Anisopteroxylon* from the Lower Miocene sediments of Mizoram, India. *Phytomorphology* 59: 1–6.

Prasad, V., A. Farooqui, S. Murthy, O. Sarate, and S. Bajpai. 2018. Palynological assemblage from the Deccan Volcanic Province, central India: Insights into early history of angiosperms and the terminal Cretaceous paleogeography of peninsular India. *Cretaceous Research* 86: 186–198.

Privé-Gill, C., C. Vozenin-Serra, S. Ducrocq, A. Naing Soe, and J.-J. Jaeger. 2004. Woods from the Pondaung Formation, Middle Eocene of Myanmar. Palaeoenvironmental implications. *Palaeontographica Abteilung B* 267: 57–65.

Quan, C., Z. Liu, T. Utescher, J. Jin, J. Shu, Y. Li, and Y.-S. Liu. 2014. Revisiting the Paleogene climate pattern of East Asia: a synthetic review. *Earth-Science Reviews* 139: 213–230.

Ramanujam, C. G. K., and M. R. R. Rao. 1966. A fossil wood resembling *Bauhinia* from the Cuddalore Series of South India. *Current Science* 35: 575–577.

Rodríguez-Reyes, O., E. Estrada-Ruiz, and P. Gasson. 2020. Evidence of large Anacardiaceae trees from the Oligocene–early Miocene Santiago Formation, Azuero, Panama. *Boletín de la Sociedad Geológica Mexicana* 72: A300719.

Rust, J., H. Singh, R. S. Rana, T. McCann, L. Singh, K. Anderson, N. Sarkar, et al. 2010. Biogeographic and evolutionary implications of a diverse paleobiota in amber from the early Eocene of India. *Proceedings of the National Academy of Sciences, USA* 107: 18360–18365.

Sahni, B. 1943. A new species of petrified palm stems, *Palmoxylon sclerodermum* sp. nov., from the Deccan Intertrappean series. *Journal of the Indian Botanical Society* 22: 209–224.

Sahni, B. 1964. Revisions of Indian fossil plants, Part III: Monocotyledons. Birbal Sahni Institute of Palaeobotany, Lucknow, India.

Sanil, M. S., S. Balakrishnan, V. B. Sreekumar, and S. A. Dev. 2022. Dipterocarps used India as a raft from Gondwana to Eurasia. *Taxon* 71: 1214–1229.

Schenk, A. 1883. Fossile Hölzer. *Palaeontographica* 30: 1–17.

Schoene, B., M. P. Eddy, K. M. Samperton, C. B. Keller, G. Keller, T. Adatte, and S. F. R. Khadri. 2019. U-Pb constraints on pulsed eruption of the Deccan Traps across the end-Cretaceous mass extinction. *Science* 363: 862–866.

Schönfeld, G. 1947. Hölzer aus dem Tertiär von Kolumbien. *Abhandlungen der Senckenbergischen Naturforschenden Gesellschaft* 475: 1–53.

Scott, R. A., and E. A. Wheeler. 1982. Fossil woods from the Eocene Clarno Formation of Oregon. *IAWA Journal* 3: 135–154.

Selmeier, A. 1993. *Moroxylon* nov. gen. (Moraceae), ein verkieseltes Maulbeerholz aus jungtertiären Schichten Bayerns (Hallertau). *Mitteilungen der Bayerischen Staatssammlung für Paläontologie und Histor. Geologie* 33: 209–226.

Selmeier, A. 1999. Kieselhölzer (*Bombax*, *Carapa*, *Cinnamomum*) aus dem untermiozänen Ortenburger Schotter, Ostmolasse Bayerns. *Mitteilungen der Bayerischen Staatssammlung für Paläontologie und historische Geologie* 39: 219–236.

Shekut, S., and A. Licht. 2020. Late Middle Miocene emergence of the Olympic Peninsula shown by sedimentary provenance. *Lithosphere* 2020: 7040598.

Shukla, A., R. C. Mehrotra, and J. S. Guleria. 2013. African elements (fossil woods) from the upper Cenozoic sediments of western India and their palaeoecological and phytogeographical significance. *Alcheringa: An Australasian Journal of Palaeontology* 37: 1–18.

Silva, M. d. S., D. M. G. Apgaua, C. C. S. Silva, L. B. da Silva, and D. Y. P. Tng. 2021. Expanding the wood anatomy economics spectrum: the correlates of vessel element lengths and pit apertures sizes in tropical forest trees. *Plant Ecology & Diversity* 14: 279–291.

Speijer, R. P. 2003. Danian-Selandian sea-level change and biotic excursion on the southern Tethyan margin (Egypt). *In* S. L. Wing, P. D. Gingerich, B. Schmitz, and E. Thomas [eds.], Causes and consequences of globally warm climates in the early Paleogene. Geological Society of America Special Papers 369: 275–290.

Srivastava, R., R. B. Miller, and P. Baas. 2019. More Malpighiales: Woods of Achariaceae and/or Salicaceae from the Deccan Intertrappean beds, India. *Journal of Systematics and Evolution* 57: 200–208.

Srivastava, R., and R. K. Saxena. 1998. Carbonised woods from the Sindhudurg Formation (Miocene) in Ratnagiri and Sindhudurg districts, Maharashtra, India. *Geophytology* 27: 23–31.

Srivastava, R., G. Srivastava, and D. L. Dilcher. 2014. Coryphoid palm leaf fossils from the Maastrichtian–Danian of Central India with remarks on phytogeography of the Coryphoideae (Arecaceae). *PLoS One* 9: e111738.

ter Welle, B. J. H., J. Koek-Noorman, and S. M. C. Topper. 1986a. The systematic wood anatomy of the Moraceae (Urticales) IV. Genera of the tribe Moreae with urticaceous stamens. *IAWA Journal* 7: 91–128.

ter Welle, B. J. H., J. Koek-Noorman, and S. M. C. Topper. 1986b. The systematic wood anatomy of the Moraceae (Urticales) V. Genera of the tribe Moreae without urticaceous stamens. *IAWA Journal* 7: 175–193.

Thomas, R. 2011a. Anatomie comparée des palmiers - Identification assistée par ordinateur, applications en paléobotanique et en archéobotanique. Ph.D. dissertation, Muséum national d'Histoire naturelle, Paris, France.

Thomas, R. 2011b. Palm-ID, a database to identify the palm stem anatomy with an expert system (Xper3). Sorbonne Université, Muséum national d'Histoire naturelle, Paris, France. Website: http://lis-upmc.snv.jussieu.fr/Palm-ID/index.html [accessed 14 March 2023].

Thomas, R., and A. Boura. 2015. Palm stem anatomy: phylogenetic or climatic signal?: Palm stem anatomy. *Botanical Journal of the Linnean Society* 178: 467–488.

Thomas, R., and D. De Franceschi. 2013. Palm stem anatomy and computer-aided identification: The Coryphoideae (Arecaceae). *American Journal of Botany* 100: 289–313.

Tomlinson, P. B., J. W. Horn, and J. B. Fisher. 2011. The anatomy of palms: Arecaceae - Palmae. Oxford University Press, NY, NY, USA.

Tosal, A., J. Pàmies, and C. Martín-Closas. 2022. Plant taphonomy and palaeoecology of Pennsylvanian wetlands from the Erillcastell Basin of the eastern Pyrenees, Catalonia, Spain. *Palaeogeography, Palaeoclimatology, Palaeoecology* 605: 111234.

Trivedi, B. S., and M. Panjwani. 1986. Fossil wood of *Bauhinia* from the Siwalik Beds of Kalagarh, U.P. *Geophytology* 16: 66–69.

Vadala, A. J., and D. R. Greenwood. 2001. Australian Paleogene vegetation and environment: evidence for palaeo-Gondwanan elements in the fossil records of Lauraceae and Proteaceae. *In* I. Metcalfe, J. M. B. Smith, M. Morwood, and I. Davidson [eds.], Faunal and floral migrations and evolution in SE Asia-Australasia, 201–226. Swets & Zeitlinger, Lisse, Netherlands.

Weeks, A., F. Zapata, S. K. Pell, D. C. Daly, J. D. Mitchell, and P. V. A. Fine. 2014. To move or to evolve: contrasting patterns of intercontinental connectivity and climatic niche evolution in 'Terebinthaceae' (Anacardiaceae and Burseraceae). *Frontiers in Genetics* 5: 409.

Westerweel, J. 2020. The India-Asia collision from the perspective of Myanmar: insights from paleomagnetism and paleogeographic reconstructions. Ph.D. dissertation, Université Rennes 1, Rennes, France.

Westerweel, J., P. Roperch, A. Licht, G. Dupont-Nivet, Z. Win, F. Poblete, G. Ruffet, et al. 2019. Burma Terrane part of the Trans-Tethyan arc during collision with India according to palaeomagnetic data. *Nature Geoscience* 12: 863–868.

Wheeler, E. A. 2011. Inside Wood – A Web resource for hardwood anatomy. *IAWA Journal* 32: 199–211.

Wheeler, E. A., and P. Baas. 2019. Wood evolution: Baileyan trends and functional traits in the fossil record. *IAWA Journal* 40: 488–529.

Wheeler, E. A., P. Baas, and S. Rodgers. 2007. Variations in dicot wood anatomy: A global analysis based on the InsideWood Database. *IAWA Journal* 28: 229–258.

Wheeler, E. A., P. K. Brown, and A. J. Koch. 2019. Late Paleocene woods from Cherokee Ranch, Colorado, U.S.A. *Rocky Mountain Geology* 54: 33–46.

Wheeler, E. A., P. E. Gasson, and P. Baas. 2020. Using the InsideWood web site: Potentials and pitfalls. *IAWA Journal* 41: 412–462.

Wheeler, E. A., and T. M. Lehman. 2009. New Late Cretaceous and Paleocene dicot woods of Big Bend National Park, Texas and review of Cretaceous wood characteristics. *IAWA Journal* 30: 293–318.

Wheeler, E. A., and S. R. Manchester. 2002. Woods of the Middle Eocene Nut Beds Flora, Clarno Formation, Oregon, USA. *IAWA Journal Supplement* 6: 188.

Wheeler, E. A., R. Srivastava, S. R. Manchester, P. Baas, and M. Wiemann. 2017. Surprisingly modern Latest Cretaceous–earliest Paleocene woods of India. *IAWA Journal* 38: 456–542.

Williams, C. J., B. A. LePage, A. H. Johnson, and D. R. Vann. 2009. Structure, biomass, and productivity of a Late Paleocene Arctic forest. *Proceedings of the Academy of Natural Sciences of Philadelphia* 158: 107–127.

Wing, S. L., F. Herrera, C. A. Jaramillo, C. Gómez-Navarro, P. Wilf, and C. C. Labandeira. 2009. Late Paleocene fossils from the Cerrejón Formation, Colombia, are the earliest record of Neotropical rainforest. *Proceedings of the National Academy of Sciences, USA* 106: 18627–18632.

Zachos, J. C., G. R. Dickens, and R. E. Zeebe. 2008. An early Cenozoic perspective on greenhouse warming and carbon-cycle dynamics. *Nature* 451: 279–283.

Zachos, J., M. Pagani, L. Sloan, E. Thomas, and K. Billups. 2001. Trends, rhythms, and aberrations in global climate 65 Ma to present. *Science* 292: 686–693.

Zerega, N. J. C., W. L. Clement, S. L. Datwyler, and G. D. Weiblen. 2005. Biogeography and divergence times in the mulberry family (Moraceae). *Molecular Phylogenetics and Evolution* 37: 402–416.

Zona, S. 2004. Raphides in palm embryos and their systematic distribution. *Annals of Botany* 93: 415–421.

SUPPORTING INFORMATION

Additional supporting information can be found online in the Supporting Information section at the end of this article.

APPENDIX S1. Dating of the Paunggyi Formation.

APPENDIX S2. Table of main features of most of the fossil Meliaceae.

How to cite this article: Gentis, N., A. Licht, D. De Franceschi, Z. Win, D. W. Aung, G. Dupont-Nivet, and A. Boura. 2024. First fossil woods and palm stems from the mid-Paleocene of Myanmar and implications for biogeography and wood anatomy. *American Journal of Botany* 111(1): e16259. https://doi.org/10.1002/ajb2.16259

Appendix 1. Correspondences between field numbers, the MNHN.F specimen numbers cited in the article and the pages on https://science.mnhn.fr.

Specimen field no.	Specimen no. for corresponding slides
PPP3	MNHN.F.50226.1, 50226.2, 50226.3
PPP4	MNHN.F.50227.1, 50227.2, 50227.3, 50227.4
PPP0	MNHN.F.50228, 50228.2, 50228.3, 50228.4, 50228.5, 50228.6
PPP9	MNHN.50229.1, 50229.2, 50229.3, 50229.4, 50229.5, 50229.6
PPP2	MNHN.50230.1, 50230.2, 50230.3, 50230.4, 50230.5, 50230.6
PPP6	MNHN.F.50231.1, 50231.2, 50231.3, 50231.4, 50231.5, 50231.6, 50231.7
PPP5	MNHN.F.50232.1, 50232.2, 50232.3, 50232.4, 50232.5, 50232.6
PPP7	MNHN.F.50233.1, 50233.2, 50233.3, 50233.4, 50233.5, 50233.6, 50233.7, 50233.8
PPP8	MNHN.F.50234.1, 50234.2, 50234.3, 50234.4, 50234.5, 50234.6
PPP10	MNHN.F.50235.1, 50235.2, 50235.3, 50235.4, 50235.5, 50235.6
PPP1	MNHN.F.50236.1, 50236.2, 50236.3, 50236.4, 50236.5, 50236.6